GEOMAR REPORT

GEOMAR

Helmholtz-Zentrum für Ozeanforschung Kiel

RV POSEIDON
Fahrtbericht / Cruise Report
POS430, POS440, POS460 & POS467

Seismic Hazards to the Southwest of Portugal

POS430 - La-Seyne-sur-Mer - Portimao (7.4. - 14.4.2012)
POS440 - Lisbon - Faro (12.10. - 19.10.2012)
POS460 - Funchal - Portimao (5.10. - 14.10.2013)
POS467 - Funchal - Portimao (21.3. - 27.3.2014)

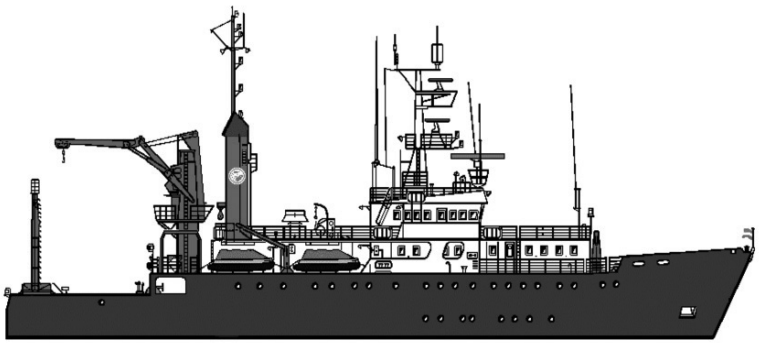

Berichte aus dem GEOMAR
Helmholtz-Zentrum für Ozeanforschung Kiel

Nr. 24 (N. Ser.)

Juni 2015

GEOMAR

Helmholtz-Zentrum für Ozeanforschung Kiel

RV POSEIDON
Fahrtbericht / Cruise Report
POS430, POS440, POS460 & POS467

Seismic Hazards to the Southwest of Portugal

POS430 - La-Seyne-sur-Mer - Portimao (7.4. - 14.4.2012)
POS440 - Lisbon - Faro (12.10. - 19.10.2012)
POS460 - Funchal - Portimao (5.10. - 14.10.2013)
POS467 - Funchal - Portimao (21.3. - 27.3.2014)

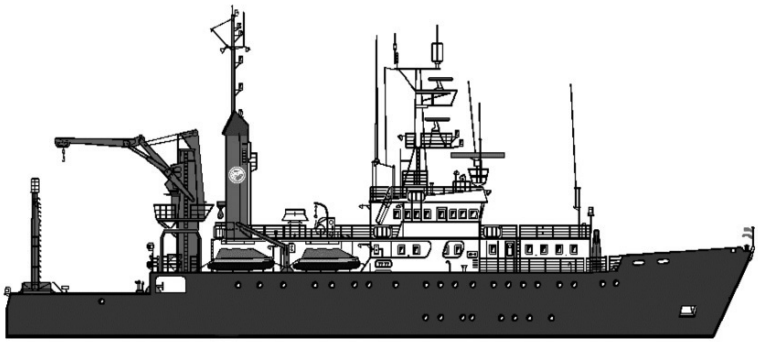

Berichte aus dem GEOMAR
Helmholtz-Zentrum für Ozeanforschung Kiel

Nr. 24 (N. Ser.)

ISSN Nr.: 2193-8113

GEOMAR
Helmholtz-Zentrum für Ozeanforschung Kiel

Das GEOMAR Helmholtz-Zentrum für Ozeanforschung Kiel ist Mitglied der Helmholtz-Gemeinschaft Deutscher Forschungszentren e.V.

The GEOMAR Helmholtz Centre for Ocean Research Kiel is a member of the Helmholtz Association of German Research Centres

Herausgeber / Editor:
Ingo Grevemeyer

GEOMAR Report
ISSN Nr. 2193-8113, DOI 10.3289/GEOMAR_REP_NS_24_2015

Helmholtz-Zentrum für Ozeanforschung Kiel / Helmholtz Centre for Ocean Research Kiel
GEOMAR
Dienstgebäude Westufer / West Shore Building
Düsternbrooker Weg 20
D-24105 Kiel
Germany

Helmholtz-Zentrum für Ozeanforschung Kiel / Helmholtz Centre for Ocean Research Kiel
GEOMAR
Dienstgebäude Ostufer / East Shore Building
Wischhofstr. 1-3
D-24148 Kiel
Germany

Tel.: +49 431 600-0
Fax: +49 431 600-2805
www.geomar.de

Table of Contents

1.1 Summary

The plate boundary at the eastern terminus of the Azores-Gibraltar transform fault between Africa and Iberia is poorly defined (Fig. 1.1). The deformation in the area is forced by the slow NW-SE convergence of 4 mm/yr between the oceanic domains of Iberia/Eurasia and Africa and is accommodated over a 200-300 km broad tectonically-active deformation zone. The region, however, is also characterized by large earthquakes and tsunamis, such as the 1969 Mw=7.9 Horseshoe Abyssal Plain earthquake and the November 1, 1755 Great Lisbon earthquake with an estimated magnitude of Mw~8.5. The exact location of the source of the 1755 Lisbon earthquake is still unknown. Recent work may suggest that the event occurred in the vicinity of the Horseshoe fault, an oblique thrust fault. In addition, the Gorringe Bank, a ~180 km-long and ~70 km-wide ridge with a relieve of ~5000 m, has been considered being a potential source of the Lisbon earthquake. Deep Sea Drilling (DSDP) and rock samples indicated that the bank is mainly composed of serpentinized peridotites with gabbroic intrusions, perhaps being created by overthrusting of the Horseshoe Abyssal Plain onto the Tagus Abyssal Plain in NW direction. Further, the Horseshoe Abyssal Plain is marked by the presence of compressive structures with a roughly NE-SW orientation and E-W trending, segmented, crustal-scale, strike slip faults that extend from the Gorringe Bank to the Gibraltar Arc in the eastern Gulf of Cadiz, which were called "South West Iberian Margin" or SWIM faults. The fault system may mark a developing Eurasia-Africa plate boundary.

Two local seismic networks were operated in the area to investigate natural seismicity and seismic harards. First, a network of 14 ocean-bottom seismometers (OBS) was operated between April and October 2012 in the vicinity of the Horseshoe fault between 10°W to 11°W, and 35°50'N to 36°10'N. OBS were deployed during RV *Poseidon* cruise POS430 and recovered during cruise POS440. From October 2013 to March 2014 a second network of 15 OBS monitored seismicity at the Gorringe Bank. OBS were deployed during RV *Poseidon* cruise POS460 and recovered during cruise POS467. Both networks benefitted from seismic stations operated in Portugal and provided in the order of 50 to 90 locale earthquakes occurring within or in the vicinity of each network. Most earthquakes in the Horseshoe Abyssal Plain occurred at a depth of 40-50 km, either in oceanic mantle or unroofed continental mantle. The large source depth of events observed in the Horseshoe Abyssal Plain supports the idea that large catastrophic earthquakes, like the Great Lisbon earthquake of 1755, may indeed occur in the area. At the Gorringe Bank seismicity was generally shallower, occurring at <30 km depth.

Zusammenfassung

Die Plattengrenze zwischen Eurasien und Afrika ist am östlichen Ende der Azoren-Gibraltar Transformverwerfung nicht eindeutig definiert. Der Grund hierfür ist eine verteilte Deformation, welche sich über eine ca. 200-300 km breite Region erstreckt und durch die NW-SE Konvergenz von Eurasien und Afrika bedingt wird. In dieser Region finden immer wieder große katastrophale Erdbeben statt. Jüngstes Beispiel ist das M=7.9 Erdbeben von 1969, welches in der Horseshoe (engl. für Hufeisen) Tiefseeebene stattfand. Das wohl prominenteste Erdbeben ist das Große M=8.5 Lissabon Erdbeben von 1755, dessen genau Quellregion bis heute unbekannt ist. Jüngere Arbeiten vermuten, dass das Lissabon Erdbeben an der Horseshoe Verwerfung, einer Überschiebungszone mit Blattverschiebungsanteil, stattfand. Als weitere potentiale Quelle wird die ca. 180 km lange und 70 km breite Gorringe Bank diskutiert, welche mit ca. 5000 m Relief die größte Struktur in der Region ist. Gesteinsproben von der Gorringe Bank deuten darauf hin, dass sie größten Teils aus Mantelgesteinen und gabbroiden Intrusionen zusammengesetzt ist und vermutlich durch die Aufschiebung der Horseshoe Tiefseeebene auf die Tagus Tiefseeebene gebildet wurde. Darüber hinaus ist die Region durch prominente Blattverschiebungszonen durchschnitten (die sog. SWIM Verwerfungen), welche in E-W Richtung verlaufen und von einigen Wissenschaftlern mit einer sich entwickelnden Plattengrenze in Verbindung gebracht werden.

In dieser durch seismische Naturgefahren bedrohten Region wurden zwei seismische Netzwerke ausgelegt, um die natürliche Seismizität und seismische Gefahrenpotential zu untersuchen. Das erste Netzwerk, bestehen aus 14 Ozean-Boden-Seismometern (OBS), wurde zwischen April und Oktober 2012 im Bereich der Horseshoe Verwerfungszone zwischen 10°W und 11°E und 35°50'N und 36°10'N ausgelegt. Die OBS wurden auf der Reise POS430 des FS *Poseidon* ausgelegt und später auf der Reise POS440 wieder geborgen. Zwischen Oktober 2013 und März 2014 wurde das zweite Netzwerk an der Gorringe Bank betrieben. Insgesamt 15 OBS wurden auf der Reise POS460 mit dem FS *Poseidon* ausgelegt und auf der Expedition POS467 aufgenommen. Beide seismische Netzwerke wurden durch seismische Stationen in Portugal und im Gibraltar-Bogen komplettiert. Beide Netze konnten zwischen 50 und 80 lokale Erdbeben registrieren, wobei die meisten Beben innerhalb bzw. in unmittelbarer der Nähe zu den Netzwerken stattfanden. In der Tiefseeebene fanden die Beben in Tiefen von 40-50 km statt. Die großen Herdtiefen deuten darauf hin, dass die Beben im Erdmantel stattfanden. Darüber hinaus stützen sie die Vorstellung, dass die Region in der Tat große Beben wie das Lissabon Erdbeben von 1755 hervorrufen kann. Beben im Bereich der Gorringe Bank waren mit 20-30 km deutlich flacher.

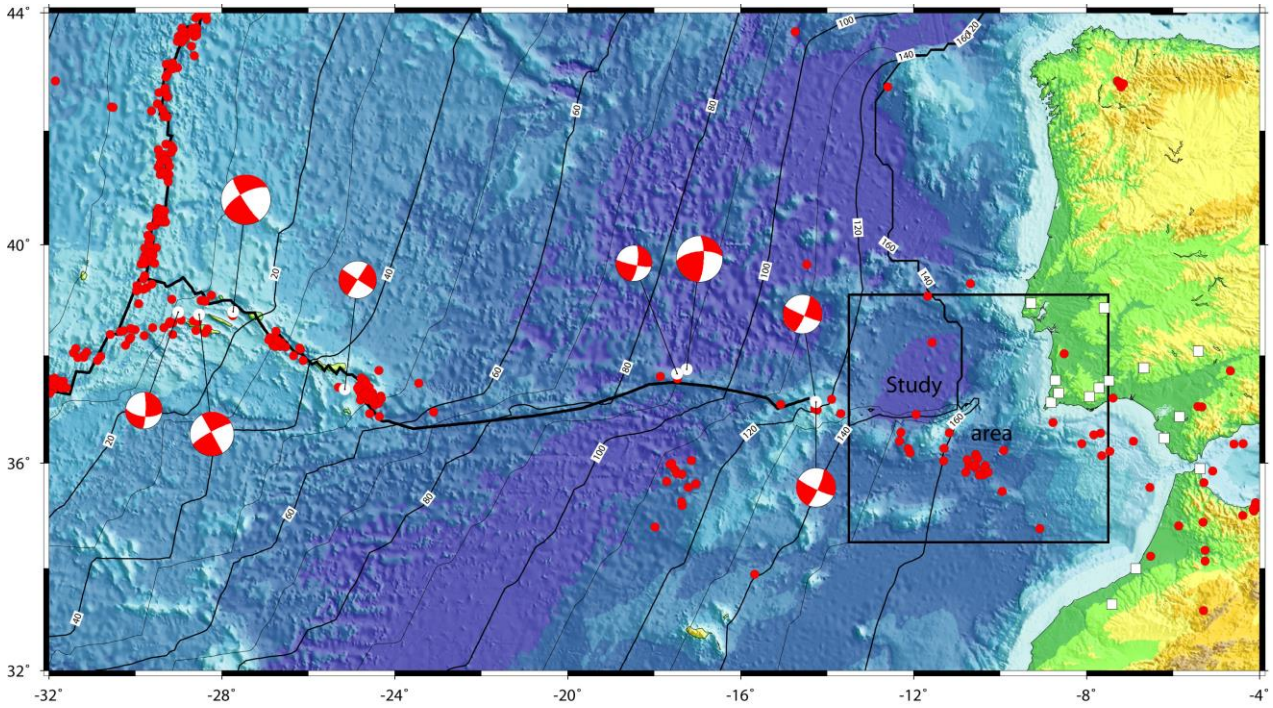

Fig 1.1.: Tectonic setting of the Gorringe Bank and Horseshoe Abyssal Plain to the SW of Portugal, were two seismic monitoring networks surveyed the local seismicity in the Horseshoe Abyssal Plain between April 2012 to October 2012 and at the Gorringe Bank between October 2013 and March 2014. The Gloria Fault, reaching from the Azores to ~14°W, defines a strike slip transform boundary. Farther, east the seismicity is distributed over a larger area and a well-defined plate boundary could not be found.

2. Scientific Prospectus and Aims

2.1. Introduction

The plate boundary between Eurasia and Africa is reasonably well defined between the Azores and the area to the west of latitude 14°W (Fig. 1.1). However, approaching the Gorringe Back near latitude 12°W the plate boundary is poorly defined. Thus, the area to the southwest of Portugal, including the Gulf of Cadiz, the Horseshoe Abyssal Plain (HASP) and the Gorringe Bank, is characterized by diffuse seismic and tectonic activity and the region lacks a clear plate boundary fault separating Africa from Eurasia/Iberia. This area hosted with the Great Lisbon earthquake of 1755 the largest known European earthquake. However, the exact location of the source of the 1755 Lisbon earthquake is still unknown. Recent evidence indicated that the event may have occurred in the vicinity of the Horseshoe fault, an oblique thrust fault. The Horseshoe fault is cut by prominent features in the bathymetry – the **S**outh-**W**est-**I**beria-**M**argin (SWIM) lineaments. The SWIM lineaments are believed to facilitate fluid migration. To study seismicity and seismic hazards, we issued the German Science Foundation (DFG) funded project GR1964/15-1 with the acronym QED for "The **Q**uest for the source area of the 1755 Lisbon **E**arthquake - revealing the maximum **D**epth of seismogenic faulting in the Horseshoe abyssal plain". The project had two main aims: (i) surveying the seismogenic potential of the area by yielding the maximum depth of seismogenic faulting and (ii) relating fluid seepage to seismically active faults. Due to the fact that seismic magnitude scales with the size of a fault zone, the maximum depth of seismogenic faulting is an important parameter to assess potential future earthquakes hazards. Thus, a greater depth would cause a potentially larger fault plain. The DFG funded project QED supported in 2012 the cruises POS430 and POS440 of the RV *Poseidon* for the deployment and recovery of a network of ocean-bottom-seismometers (OBS) in the vicinity of the Horseshoe Fault and the SWIM lineaments.

In 2013 - on short notice - ship time became available as the cruise POS461 in to the Aegean Sea had been cancelled due to problems with the research permit in an area where both Greece and Turkey have claims. Therefore, the GEOMAR Helmholtz Research Centre funded within the framework of its OCEANS programme the operation of a second seismic network at the Gorringe Bank, an area being among the potential source areas of the Great Lisbon earthquake of 1755. We called the project QED II; network installation occurred during RV *Poseidon* cruise POS460 in 2013, recovery of seismic stations was conducted during the cruise POS467 in 2014.

2.2 Scientific Background

The study area corresponds to the eastern segment of the Azores-Gibraltar plate boundary between Gorringe Bank to the West, the Coral Patch Ridge to the South and the accretionary prism of the Gulf of Cadiz to the East (Fig. 2.1 + 2.2). In this area, the plate boundary is poorly defined. The deformation is forced by the slow NW-SE convergence (4mm/year; *Argus et al.*, 1989) between the oceanic domains of the Eurasia and Africa plates and is accommodated over a 200-300 km broad tectonically-active deformation zone (*Sartori et al.*, 1994; *Hayward et al.*, 1999; *Buffon et al.*, 2004). This type of diffuse plate boundary is analogous to the intraplate deformation identified in the Indian Ocean (*Wiens et al.*, 1985). The region is also characterized by large earthquakes and tsunamis, such as the 1969 Mw=7.9 Horseshoe Abyssal Plain earthquake (*Fukao*, 1973) and the November 1, 1755 Great Lisbon earthquake with an estimated magnitude of Mw~8.5 (*Martinez-Solares et al.*, 1979; *Johnston*, 1996). However, the location of the source area of the Great Lisbon earthquake is still under controversial debate. A number of features have been suggested, including the Gorringe Bank (e.g., *Johnston*, 1996), the Marques de Pombal fault (e.g., *Zitellini et al.*, 2001; *Garcia et al.*, 2003), and a proposed subduction megathurst in the Gulf of Cadiz (*Gutscher et al.*, 2002). However, tsunami parameters suggest that the source was to the southwest of Cape Sao Vincente (*Batiza et al.*, 1998). The Horseshoe Abyssal Plain and the Horseshoe fault are therefore considered as being the most likely location of the source of the Great Lisbon earthquake (*Stich et al.*, 2007).

The region is marked by the presence of compressive structures with a roughly NE-SW orientation (*Sartori et al.*, 1994; *Hayward et al.*, 1999) and E-W trending, segmented, crustal-scale, strike slip faults that extend from Gorringe Bank to the Gibraltar area in the eastern Gulf of Cadiz ("South West Iberian Margin - SWIM" faults; *Zitellini et al.*, 2009; *Rosas et al.*, 2009; *Duarte et al.*, 2009). *Zitellini et al.* (2009) suggested that these faults mark a developing Eurasia-Africa plate boundary. The SWIM lineaments (Fig. 2.1) correspond to the bathymetric expressions of the reactivation of WNW-ESE-pre-existing faults (*Rosas et al.*, 2009). In particular, the lineaments passing through the area consist of a network of shear structures that evokes the development of an incipient strike-slip fault system.

Fault zones are known to provide fluid migration pathways in convergent settings (*Moore and Vrolijk*, 1992). Widespread mud volcanism occurs in the Gulf of Cadiz sedimentary wedge, often located along SWIM lineaments (*Hensen et al.*, 2007; *Scholz et al.*, 2009). The geochemical signature of fluids indicate that some component originated in the igneous basement (*Hensen et al.*, 2007), suggesting that faults reach though the sedimentary sequence down to the basement. To keep those pathways open, faults have to be active.

The Mio-Quaternary sedimentary prism of the Gulf of Cadiz was initially emplaced as part of the Gibraltar orogenic arc. The sediments are extensively folded and faulted as a consequence of tectonic activity in the region, with the central part being an accretionary wedge (Fig. 2.1). It is currently debated whether subduction is still active (e.g., *Gutscher et al.*, 2002) or whether the westward motion of the

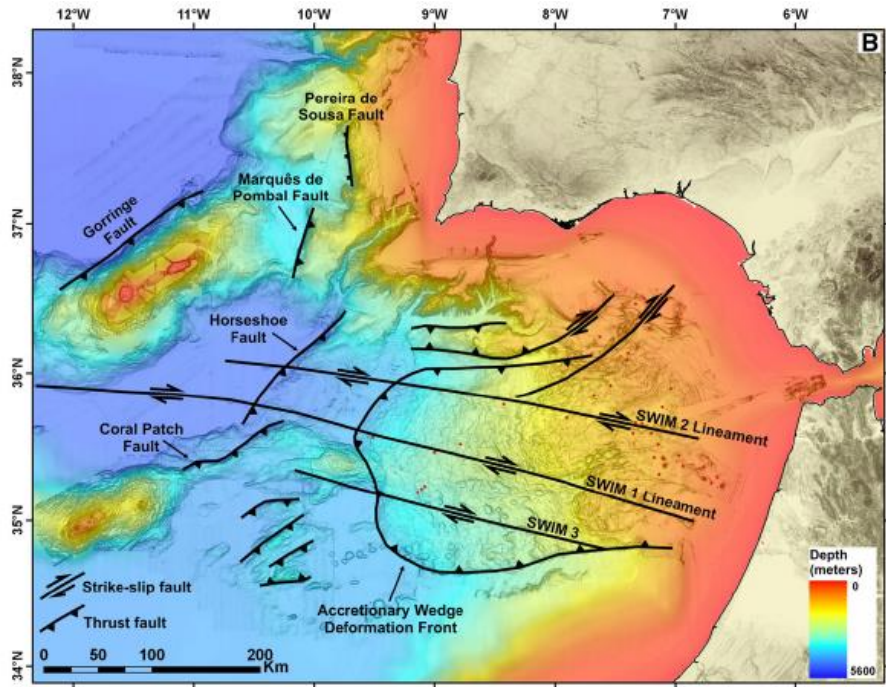

Fig 2.1. Multi-beam bathymetry (Zitellini et al., 2009) and main tectonic features of the Gulf of Cadiz and the Horseshoe abyssal plain (after Duarte et al., 2009).

wedge is at present related to the transpressive Eurasia-Africa plate boundary (e.g., *Zitellini et al.*, 2009). Heat flow data over the accretionary prism of the Gulf of Cadiz, however, support that the interpretation that subduction has largely ceased (*Grevemeyer et al.*, 2009).

Heat flow data from the Iberia margin, the Gulf of Cadiz, Horesshoe Abyssal Plain and the eastern Atlantic ocean show an unusual large scatter. Values of 45 mW/m2 have been measured over the NW Iberian Margin Ocean Drilling Program (ODP) drilling transect (*Louden et al.*, 1997) and similar values

would be expected across the Horseshoe Abyssal Plain, because it belongs to the same geological province (*Rovere et al.*, 2004*; Müller et al.*, 2008). However, previous work in the Horseshoe Abyssal Plain and to the north of Coral Patch Ridge revealed much higher heat flow values of about 60 mW/m2 (Grevemeyer et al., 2009; unpublished data from SO175). Further west, the values decrease again to much lower heat flow (<40 mW/m2) over Mesozoic oceanic crust (Fig. 2.2; red > 58 mW/m2; green >58 to >48 mW/m2; blue <48 mW/m2) where the age and nature of the crust is well constrained by seafloor spreading anomalies (e.g. *Müller et al.*, 2008). One explanation for the high heat flow values measured over the eastern Horseshoe Abyssal Plain is that widespread tectonic activity caused the mantle to fracture – consistent with the occurrence of numerous earthquakes – facilitating fluid migration to reach mantle and hence cause its serpentinization. Serpentinization is supported by low mantle velocities under the Horeshoe abyssal plain (*Rovere et al.*, 2004; *Martinez-Loriente et al.*, 2014). Serpentinization, however, is an exothermic reaction, and the additional heat (compared to regional values of ~45mW/m2) may explain the observed anomaly (Fig. 2.2). This phenomenon is documented at the Central Indian Ocean diffuse plate boundary (*Delescluse and Chamot-Rooke*, 2008). In cooperation with H. Villinger (Univ. Bremen) thermal models were calculated to assess the temperature structure of the lithosphere. Temperature versus depth for a lithosphere with 45 mW/m2 indicates a temperature of 600°C at a depth of 50 km, while a surface heat flow of 60 mW/m2 with serpentinization at mantle depth suggest that 600°C is reached at 35-40 km (Fig. 2.3). These calculations provide important constraints on the depth distribution of seismicity and the maximum depth of the seismogenic layer as earthquakes in the oceanic lithosphere are inherently related to temperatures < 600°C (e.g., *McKenzie et al.*, 2005).

Based on global travel time data the best available constraints on the source depth of earthquakes in the Horseshoe Abyssal Plain are reported in the EHB catalogue (*Engdahl et al.*, 1998). The EHB catalogue (including recent updates) suggest that earthquakes under the Horseshoe abyssal plain occur at 15 to 45

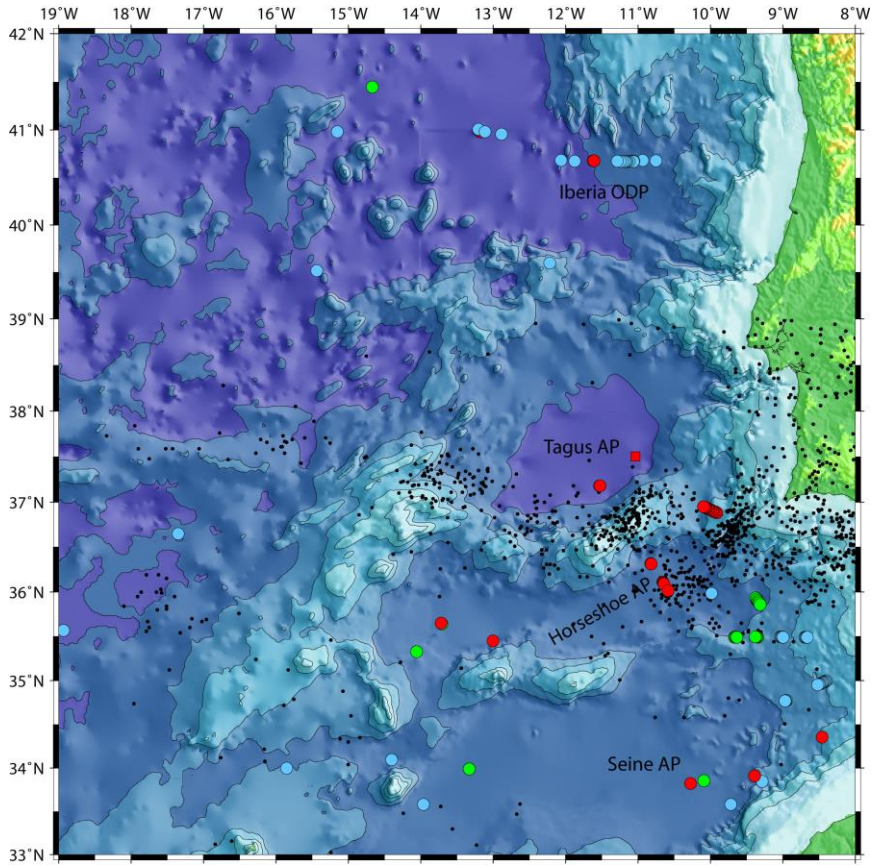

Fig 2.2. Heat flow anomalies(colored circles) to the west of Portugal and Morocco (for simplicity, anomalies are depth coded: red > 58 mW/m^2; green >58 to >48 mW/m^2; blue <48 mW/m^2). Black dots are earthquake epicenters.

km depth. The largest earthquake in the Horseshoe abyssal plain was the Mw=7.9 1969 earthquake, occurring at 33 km.

A deployment of 24 ocean bottom seismometers in the Tagus and Horseshoe Abyssal Plain and the Gulf of Cadiz (average station separation ~50 km) of the EU-NEAREST project provided events much deeper at 40-60 km (*Geissler et al.*, 2010). *Geissler et al.* (2010) suggested in their paper that this depth in consistent with the thermal state of a 140 Myr old lithosphere. However, considering measured data, we were able to show that their depth estimates clearly contradicts thermal models for the area (even the model calculated for "normal" heat flow without serpentinization – see Fig. 2.3). It is likely that the depth reported by *Geissel et al.* (2010) is strongly biased by the velocity model that has been used by the authors. The model is based on seismic refraction data from an onshore/offshore experiment in southern Portugal. However, recording of marine shots was facilitated just by land stations without any offshore seismometers (*Gonzalez et al.*, 1996). *Geissler et al.* (2010) used a 16 km thick crust and fast mantle with velocities of 8.1-8.5 km/s (see supplementary material of *Geissler et al.*, 2010). Under the Horseshoe abyssal plain, however, crust is only 4-5 km thick and mantle is with 7.4 km/s very slow (*Rovere et al.*, 2004; *Martinez-Loriente et al.*, 2014; *Valenti Sallares*, pers. communication). Using a too fast mantle instead of a slow mantle will cause a too large depth of the hypocenters, even when formal errors are small. Unfortunately, it will be difficult to improve the velocity model based on the NEAREST data, as only a handful of stations where located in the Horseshoe abyssal plain itself and a station spacing of ~50 km inherently limits the ability to resolve shallow earthquakes (depth<20-30 km) with small errors.

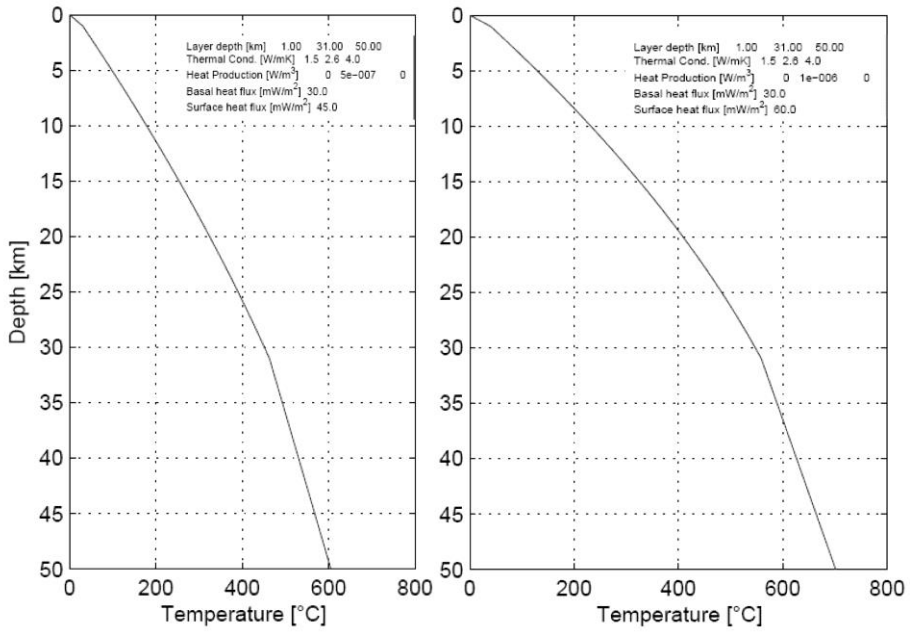

Fig. 2.3: Thermal model calculated for the Horseshoe abyssal plain. Note, seismogenic rupture is related to temperatures <600°C in the oceanic lithosphere (courtesy H. Villinger, Univ. Bremen).

In all cases the existing seismological data, even though associated with large errors, indicate that most events occur in the mantle and hence favour a seismically-driven mantle serpentinization model as supported by elevated heat flow. In contrast, most earthquakes reported worldwide occur in crustal rocks. The aim of the proposed work is to learn more about the seismic activity in the Horseshoe Abyssal Plain and to provide source parameters with small errors. This will be essential in relating centroid depth to the thermal structure and providing a more precise assessment of the maximum depth of earthquakes in the area. These information are critical to survey the seismic potential of the Horseshoe Abyssal Plain to cause large earthquakes, like the Great 1755 Lisbon earthquake.

2.3 The 2007 Horseshoe Fault Earthquake

The largest earthquake observed that occurred since the M~7.9 1969 Horseshoe Abyssal Plain earthquake was the Mw=6.0 2007 Horseshoe Fault event (e.g., *Stich et al.*, 2007). Teleseismic data can be used to constrain the rupture process and the hypocentral parameters of the event. High quality seismic waves were recorded by stations of the global broadband seismograph network, which enables a detailed characterization of the nucleating depth and rupture process using waveform inversion. Depth resolution results from the time separation between the direct P wave and the pP and sP phases; thus, waveforms are very sensitive to the time delay between the first arriving P wave and the later-arriving surface reflected phases. In this study, a sampling rate of 1 s is used, suggesting that depth resolution is limited because the minimum depth increment to be resolved by depth phases is for pP and sP on the order of 2 to 3 km (Kikuchi and Ishida, 1993).

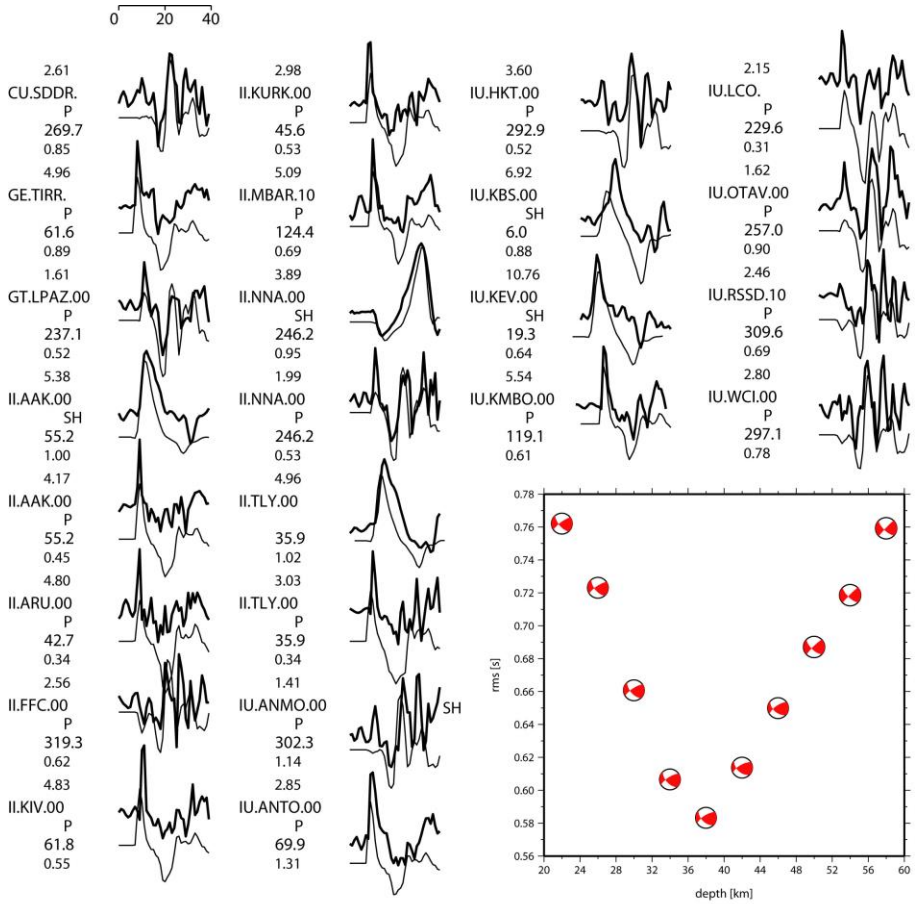

Fig. 2.4: Teleseismic waveform inversion of the Mw=6.0 2007 Horseshoe abyssal plain earthquake, indicating a centroid at 38 +/- 4 km.

We used an iterative least-squares inversion (e.g., *Kikuchi and Kanamori*, 1991; *Lefeldt and Grevemeyer*, 2007) of azimuthally distributed seismic P and SH body-wave signals from stations at distances of about 30° to 90°, yielding the rupture mechanism, depth, and source time function. Waveforms are corrected for instrument responses to obtain displacement seismograms. The inversion assumes attenuation with a t* (travel time divided by average Q) of 1 s for P waves and 4 s for SH waves. The Green functions were computed for simple layered source and receiver structures connected by geometric spreading for a deeper ak135 Earth model (*Kennett et al.*, 1995). The velocity structure at the source included a water layer overlying a half space with Vp=6.0 km/s, Vs=3.55 km/s and ρ=2.67 g/cm3. The source was fixed at the epicentre of Stich et al. (2007) (Fig. 2.5).

For the inversion, 19 P waves and 5 SH waves that provided waveforms were chosen (Fig. 2.4). The mechanism indicated dip-slip motion and a centroid depth (depth where the maximum of seismic moment was released) of 38 +/- 4 km (Fig. 2.4) and hence near the lower limit of the thermal estimate for the seismogenic layer in the Horseshoe Abyssal Plain, but much shallow than estimated in the NEAREST experiment (see 2.2 for more information).

2.4 Goals

The largest historic earthquake that ever hit Europe was the Great Lisbon earthquake of 1755, causing a great tsunami. Its source location is still under debate. Our monitoring efforts conducted to the SW of Portugal will help to improve estimates for the seismogenic potential of both the Gorringe Bank and the Horseshoe Abyssal Plain. Both settings are potential source areas of the Lisbon earthquake. The size of an earthquake is inherently related to the size of a fault zone. Thus, larger earthquakes require larger fault plains. The down-dip limit of faulting in oceanic lithosphere (or in the case of the Horseshoe Abyssal Plain perhaps continental mantle) is believed to be related to the temperature structure (e.g., *McKenzie et al*., 2005). Existing estimates suggest that faulting should be restricted to a depth of <35-40 km. However, seismic estimates show a large scatter, with different approaches defining different depth intervals (e.g., EHB indicates events < 45 km; waveform inversion of the Mw=6.0 Horseshoe earthquake indicates 35-40 km; in contrast, *Geissler et al.* (2010) suggests 40-60 km). Unfortunately, the only existing local deployment of the NEAREST experiment is limited in its ability to resolve the maximum depth, as the station separation of marine deployments was too large and the network provided a too small number of stations in the Horseshoe Abyssal Plain itself to jointly invert data for source depth and earthquake location. Further, during the NEAREST experiment a large number of OBS lost its time base, required for precise estimates of hypocentral parameters. We therefore decided to operate networks of densely spaced OBS to supplement the NEAREST network by OBS spaced at <20 km that will provided hypocentres at with much smaller location uncertainties.

The two deployments are going to address a number of goals and objectives:

1. Characterization of the minimum and maximum depth of local earthquakes

Precise estimates of earthquake locations (both in Lon/Lat and depth) will allow us to approximate the thickness of the seismogenic layer. In turn, this has important implications for the rheology and mechanical behavior of the lithosphere.

2. Defining frequency-magnitude relationship for Horseshoe earthquakes

The so called *b*-value can be used to understand and survey the frequency-size distribution of earthquakes. In the case of wide-spread serpentinization, a high *b*-value of 2 or larger might be expected, as found for bending-related earthquakes in the trench-outer rise of subduction zones (*Lefeldt et al.*, 2009). A *b*-value of 1 would indicate normal conditions.

2. Characterization of the seismic velocity structure of the Horseshoe Abyssal Plain using P- and S-waves

A large number of local earthquakes recorded on a local network can be used to invert the travel time data jointly for earthquake location and a so called minimum 1-D velocity model. If the number of local events is large enough, a 3-D velocity structure can be derived. Right now, existing active source data could not penetrate deeper than ~11 to 13 km (*Rovere et al.*, 2004; *Martinez-Loriente et al.*, 2014) and are limited in their ability to derive S-wave velocities. However, using P- and S-wave arrival times of local earthquakes the velocity structure can be resolved at larger depth, as earthquakes nucleate at least down to 35-40 km, as indicated by the Mw=6.0 Horseshoe earthquake. The Vp/Vs ratio is important for assessing the amount of serpentinization.

3. Surveying the relationship between maximum depth of seismic activity and thermal structure

Previous estimates for oceanic lithosphere suggest that faulting is limited to temperatures of <600°C. It has been proposed that the rocks underlying the Horseshoe Abyssal Plain are unroofed continental lithosphere. Does this relationship also applies for continental mantle?

4. Estimation of the strength of the lithosphere in the Horseshoe Abyssal Plain to assess the seismic hazard of a future large earthquake
The assessment of the *b*-value and the Vp/Vs ratio will provide a first assessment for the rheology and of a strong or weak mantle. The strength of the host rock is important for the frictional properties of a fault zone. In addition to the size (define by the thickness of the seismogenic layer and the length of a fault) the frictional behavior will govern the seismic moment of a future earthquake.

5. Using focal mechanism to define fault segments
Seismic reflection data revealed a number of fault zones in the Horseshoe abyssal plain. Focal mechanisms can be used to assess motion of these faults.

6. Earthquake activity and seepage
In the vicinity of the Horseshoe faults seepage and mud volcanoes were observed. It is likely that seepage will occur over active faults. The densely spaced OBS network might be able to located some local earthquakes or clusters of events that are related to faults governing fluid migration.

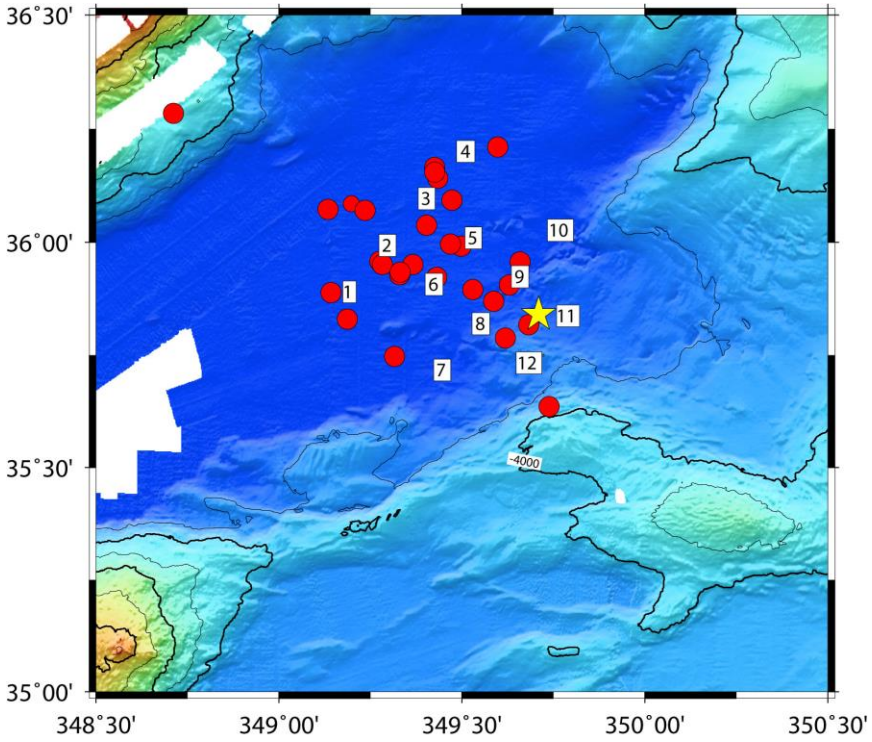

Fig. 2.5. Location map of the seismic network in the Horseshoe Abyssl Plain. Red dots are earthquakes reported in the EHB catalogue and yellow star marks the Mw=6.0 2007 earthquake at the USGS epicentre.

3. Sea-going programme

3.1 RV *Poseidon* cruise POS430

Port calls: La-Seyne-sur-Mer, France (7. April 2012)
Portimao, Portugal (14. April 2012)
Captain: Matthias Günther
Chief-Ing.: Hans-OttoStange
Chiefmate: Theo Griese

3.1.1 Narrative of the Cruise POS430

Poseidon left the harbour of La Seyne sur Mer, France on Easter Saturday the 7th of April 2012 at 18:40 local time. Due to strong northwesterly winds of 9-10 Bft and waves with a height of up to 7 m *Poseidon* had to face very rough condition during its first day at sea. In the afternoon of Easter Sunday 8th of April the condition improved after *Poseidon* left the area where the Mistral and winds from the Pyrenees affected forcefully the sea state. Around noon on April 9 *Poseidon* passed the Balearic Island of Ibiza. On 10th of April at about 10 a.m. *Poseidon* sailed around the Carbo de Gata and entered the Alboran Sea. Strong head winds of 7 to 9 Bft and heavy waves slowed down the vessel. After lunch time on 11th of April conditions improved and *Poseidon* passed Gibraltar on 17:00 local time, entering the Atlantic ocean at approx. 20:00 local time. In the beginning of Thursday 12th of April weather conditions in the Gulf of Cadiz were fine, however, approaching the deployment area wind speed increased again and reached state 7 to 8 Bft. At Thursday night at 22:58 local time (21:58 UTC) the first ocean-bottom-seismometer (OBS), station OBS01, was deployed (Fig. 3.2). Deployment continued for the next 19 hours, deploying in total 14 OBS in the Horseshoe Abysal Plain. Wind speed slowed down to 5 to 6 Bft. The last station, OBS14, was deployed at 6.09 p.m. on Friday 13th of April 2012. Thereafter, Poseidon headed towards Portimao, reaching the Portuguese port in the morning of 14th of April 2012. At 9:40 *Poseidon* was safe at the pier.

Fig. 3.1. Track chart of cruise POS430, La-Seyne-sur-Mer to Portimao.

3.1.2 Cruise participants POS430

Name	Discipline	Institution
Grevemeyer, Ingo, chief scientist	OBS	GEOMAR
Lieser, Kathrin, scientist	OBS	GEOMAR
Möller, Stefan, scientist	OBS	GEOMAR

GEOMAR Helmholtz Zentrum für Meeresforschung Kiel,
Wischhofstraße 1-3,
24148 Kiel
Germany

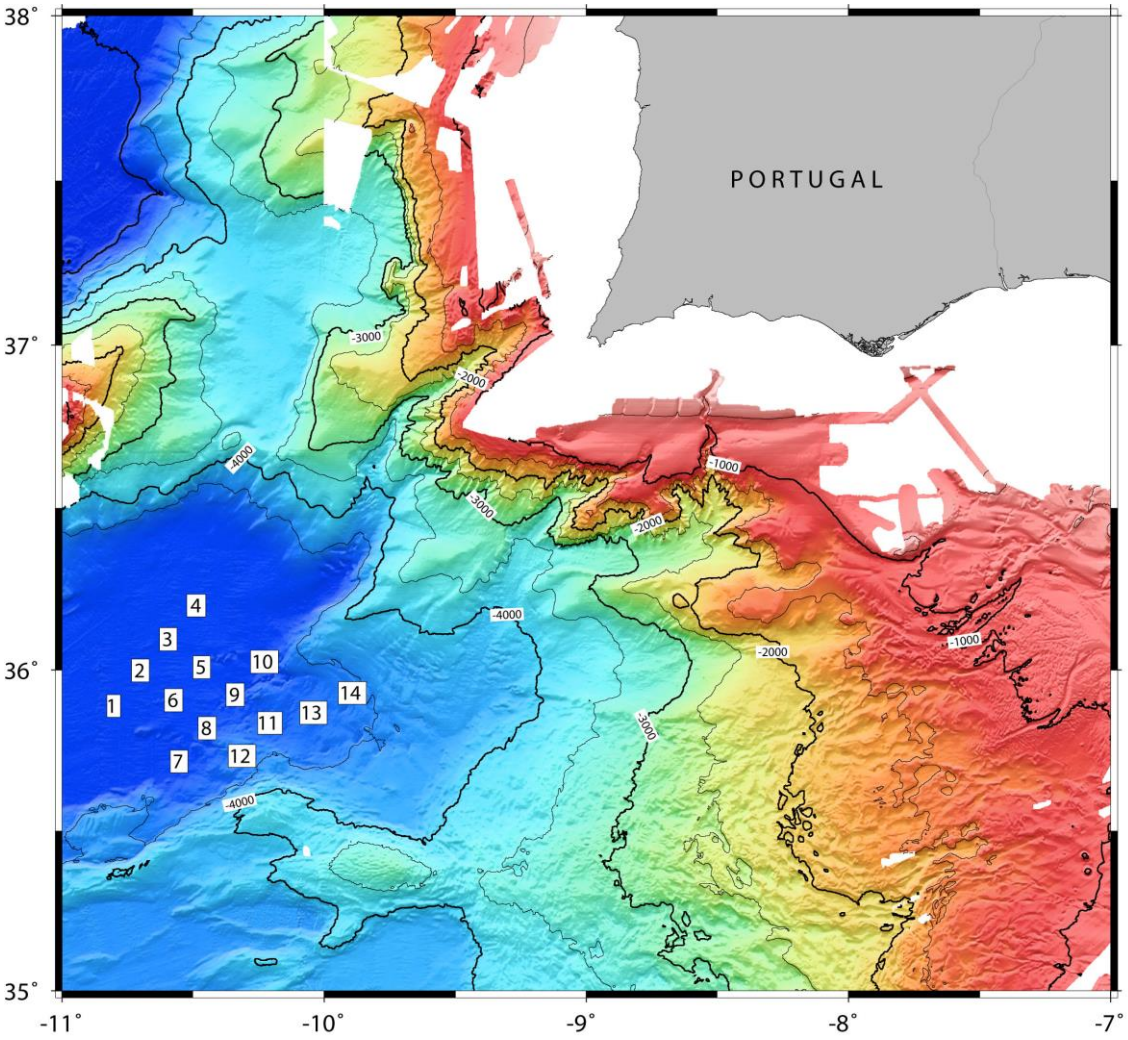

Fig. 3.2 . Network of ocean bottom seismometers (OBS) deployed in the Horseshoe Abyssal Plain and across the Horseshoe Fault, recording local earthquakes over six month.

3.2 RV *Poseidon* cruise POS440

Port calls: Lisbon, Portugal (12. October 2012)
Faro, Portugal (19. October 2012)
Captain: Bernhard Windscheid
Chief-Ing.: Kurre Kröger
Chiefmate: Theo Griese

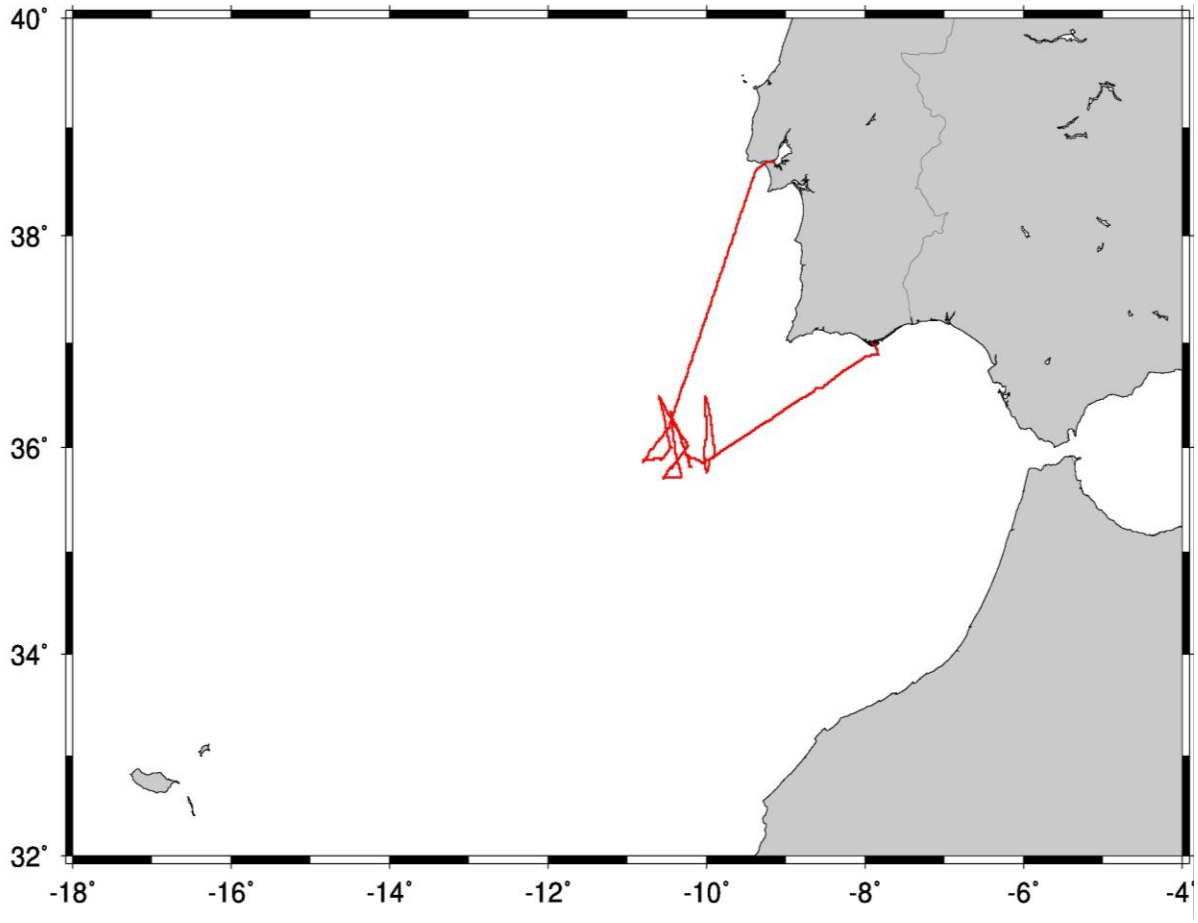

Fig. 3.3. Track chart of cruise POS440, Lisbon to Faro.

3.2.1 Narrative of the Cruise POS440

On Saturday 13th October 2012 *Poseidon* left the harbour of Lisbon, Portugal at 07:56 local time. Due to excellent weather conditions and north-westerly winds of 3-4 Bft the vessel steamed quickly south, passing Cabo Sao Vincente in the afternoon, reaching the first OBS location in the early morning of Sunday the 14th of October. The station, namely OBS04 deployed during *Poseidon* cruise POS430 in April (Fig. 3.2), was released at 7:00 local time (or 6:00 UTC) at still perfect weather conditions with a moderate Atlantic swell. 68 minutes later the OBS surfaced and was recovered 15 minutes later. During the first day in total 6 OBS were recovered, the last station, OBS05, was released at 16:46 local time, surfaced at 17:57 and was recovered at 18:08. For the night the recovery was suspended. On the night to Monday the 15th of October the wind increased to 5-6 Bft, proving relatively rough conditions in the morning. However, during the day conditions improved and the wind was just 2-4 Bft during the day. On Monday the first instrument, OBS10, was released at 8:06 local time. The instrument surfaced roughly one

hour later at 9:08 and was recovered at 9:19 local time. Over the next hours in total 5 OBS were recovered. The last station, OBS 12, was recovered at 17:17 local time and operations were again suspended for the night. During Tuesday the 16th of October weather was well again, but a longwave lengths swell occurred. At 8:08 the first instrument, OBS11, was released. Based on its radio signal we know that the station surfaced at 9:15 local time. However, we were not able to detect the instrument visually. Only after roughly half an hour we were able to catch the OBS by eye. At 9:51 local time the OBS was recovered. During the morning some decks work required operation of the large crane. This was only possible on a NNW trending course. At 11:30 crane operation was finished and the next instrument, OBS13, was released at 2:18 local time. The last seismic monitoring station, OBS14, surfaced at 13:24 and was recovered at 13:43 local time. Thus, all 14 OBS deployed during the cruise POS430 in April were successfully recovered.

Due to the unexpectedly excellent weather conditions we could finish our main program much earlier than expected. *Poseidon* run a number of mapping profiles and started at 10 a.m. on Wednesday the 17th of October its transit towards Faro. During the transit a low pressure system over the Bay of Biscay brought rough sea and rain, luckily all OBS were safe on deck. *Poseidon* reached the pilot station in the morning hours of Thursday 18th of October, waiting for high tide to reach port. At 10:30 local time *Poseidon* met the pilot and was at 11:35 safe at the pier. A successful cruise ended.

3.2.2 Cruise participants POS440

Name	Discipline	Institution
Grevemeyer, Ingo, chief scientist	OBS	GEOMAR
Steffen, Kaus-Peter, technician	OBS	GEOMAR
Möller, Stefan, scientist	OBS	GEOMAR
Corela, Carlos Jorge Caetano	OBS	IDL

GEOMAR	Helmholtz Zentrum für Meeresforschung Kiel, Wischhofstraße 1-3, 24148 Kiel Germany
IDL	Instituto D. Luiz Campo Grande, Ed. C8, piso 3 1749-016 Lisboa, Portugal

3.3 RV *Poseidon* cruise POS460

Port calls: Funchal, Madeira, Portugal (5. October 2013)
Portimao, Portugal (14. October 2013)
Captain: Bernhard Windscheid
Chief-Ing.: Hans-Otto Stange
Chiefmate: Dirk Thürsam

3.3.1 Narrative of the Cruise POS460

The research vessel *Poseidon* left the port of Funchal, Madeira on Saturday 5th of October 2013 at 09:00 local time. Facing good weather conditions and winds of 3-5 Bft *Poseidon* steamed northward sailing towards the Gorringe Bank to the southwest of Cabo Sao Vincente, the southwesternmost point of Portugal. On Monday 7th of October 2013 we reached the working area, deploying the first ocean bottom seismometer (OBS) at 8:20 local time (7:20 UTC) to the southwest of Gorringe Bank (Fig. 3.5). Over the next five days we deployed in total 15 OBS in the working area, covering the Gorringe Bank and the westernmost portion of the Horseshoe Abyssal Plain, recording continuously local earthquake until the network will be recovered during the cruise POS467 of *Poseidon*. The last OBS was deployed on Friday the 11th of October at 9:10 local time. Until Sunday morning some mapping was carried out over the Gorringe Bank. On Sunday the 13th of October at 8 a.m. local time *Poseidon* started its transit towards the Portuguese port of Portimao. On Monday 14th of October at 9:15 a.m. local time *Poseidon* met the pilot and arrived at the pier at 9:45.

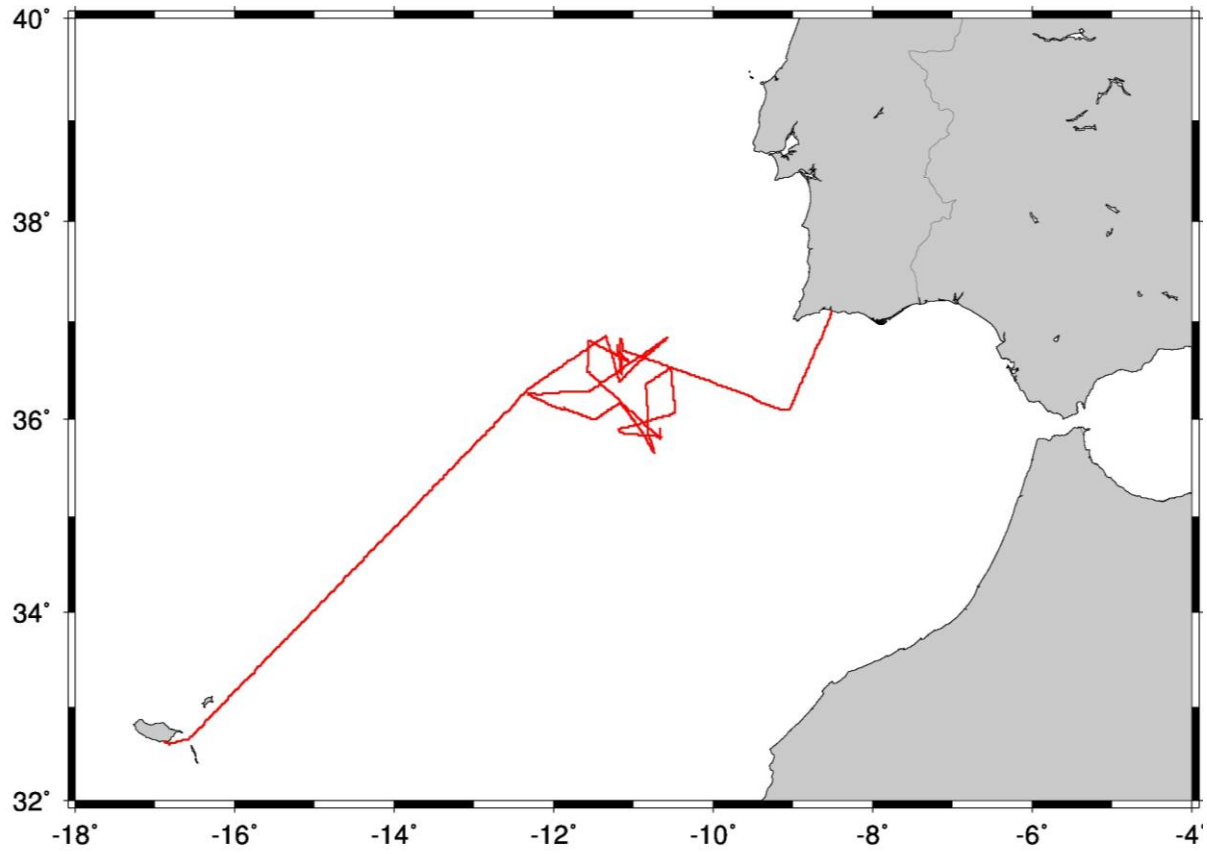

Figure 3.4. Track chart of cruise POS460, Funchal, Madeira to Portimao.

3.3.2 Cruise participants POS460

Name	Discipline	Institution
Grevemeyer, Ingo, chief scientist	OBS	GEOMAR
Lange, Dietrich, scientist	OBS	GEOMAR
Schröder, Patrick, technician	OBS	GEOMAR

GEOMAR Helmholtz Zentrum für Meeresforschung Kiel,
Wischhofstraße 1-3,
24148 Kiel
Germany

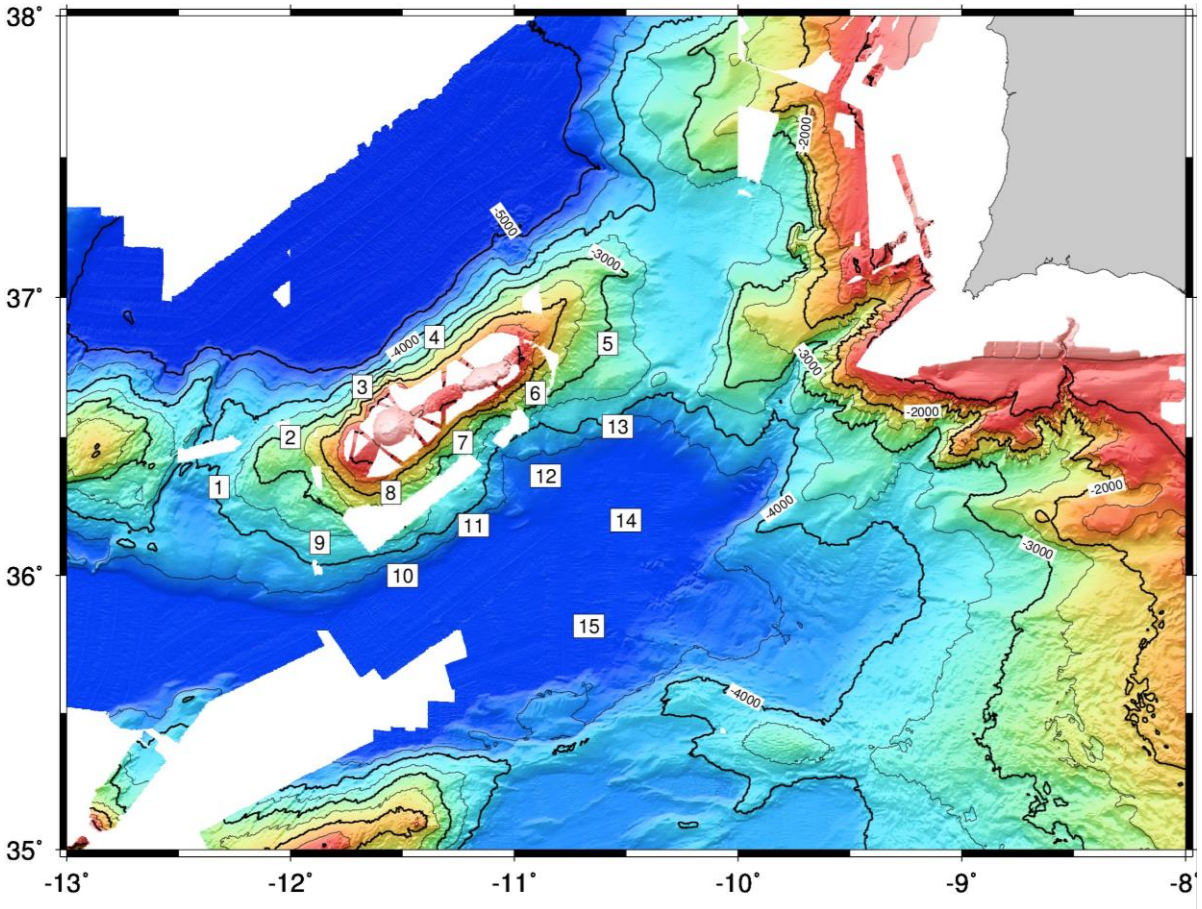

Fig. 3.5. Network of 15 ocean bottom seismometers (OBS) deployed during Poseidon cruise P460. OBS were deployed over the Gorringe Bank and in the Horseshoe Abyssal Plain, recording local earthquakes over six month.

3.4 RV *Poseidon* cruise POS467

Port calls: Funchal, Madeira, Portugal (21. March 2014)
Portimao, Portugal (27. March 2014)
Captain: Matthias Günther
Chief-Ing.: Hans-Otto Stange
Chiefmate: Theo Griese

3.4.1 Narrative of the Cruise POS465

On Friday 21st of March 2014 the research vessel *Poseidon* left the port of Funchal at 09:00 local time, aiming to recover ocean-bottom-seismometers (OBS) deployed during the cruise POS460 in autumn of 2013 at the Gorringe Bank to the SW of Portugal (Fig. 3.5). During the transit to the Gorrigne Back we had very good conditions, sunny weather and winds of 3-5 Bft. After a transit of about two days *Poseidon* reach the first OBS location. At 7:05 a.m. local time (UTC) on the 23rd of March we sent the first release command, calling OBS01 back to the surface. About one hour later, the OBS surfaced at 8:07 and only 11 minutes later the OBS was recovered and on deck. During the 23rd we recovered four OBS (OBS01 to OBS04). During night times, the recovery was suspended. Weather conditions during the recovery were fair, with winds of up to 7 Bft and waves of up to 5.5 m. However, deck's operations were hardly affected by the weather. On the 24th of March the same procedure followed, recovering OBS05 at 8:18, and three additional stations over the next hours until darkness approached. On the 25th of March OBS09 to OBS12 were recovered. OBS12 was safely back on deck at 5:36 p.m. The last three remaining OBS were planned to be recovered on the 26th of March. At 9:47 OBS13 was on deck and OBS 14 was recovered at 13:16. At 3:24 p.m. we tried releasing OBS15. Unfortunately, we neither received any answer from it nor did the OBS surface. We remained at the site for about 3 hours and tried to release it a number of times. At 18:30 we had to stop the recovery operation and began our transit towards Portimao. On Thursday the 27th of March 2015 *Poseidon* reached the port of Portimao on the Algarve coast.

3.4.2 Cruise participants POS467

Name	Discipline	Institution
Grevemeyer, Ingo, chief scientist	OBS	GEOMAR
Lange, Dietrich, scientist	OBS	GEOMAR
Schröder, Patrick, technician	OBS	GEOMAR
Schippkus, Sven, student	OBS	CAU

GEOMAR Helmholtz Zentrum für Meeresforschung Kiel,
Wischhofstraße 1-3,
24148 Kiel
Germany

CAU Institut für Geowissenschaften, Christian-Albrechts Universität Kiel,
Otto Hahn Platz, 24108 Kiel, Germany

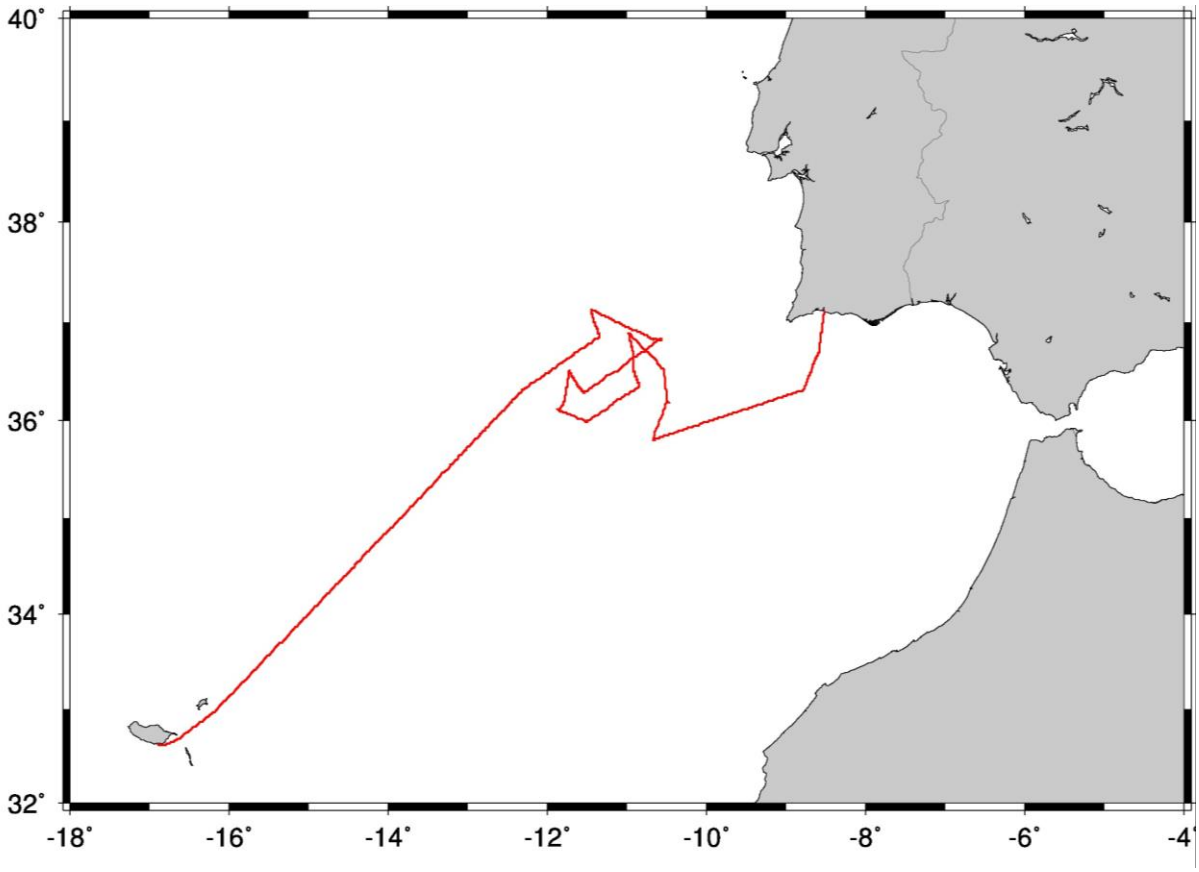

Figure 3.6. Track chart of cruise POS467, Funchal, Madeira to Portimao.

4. Scientific equipment – Ocean Bottom Seismometers

GEOMAR operates Ocean Bottom Hydrophones (OBH) since January 1992. This type of instrument has proved to have a high reliability; more than 4500 successful deployments were conducted since 1992. For both deployments, 14 to 15 short period OBS were available. Thus, in total 29 stations provided long-term earthquake monitoring data for about 6 month from the Horseshoe Abyssal Plain and the Gorringe Bank.

The OBS are a joint GEOMAR and *KUM* GmbH design for long-term seismological observations. Syntactic foam is used as floatation body (Fig. 4.1). The release transponder is a model *K/MT562* made by *KUM GmbH*. The recording unit is hosted in a titanium pressure tube. Seismic sleuth are recorded by a hydrophone and a seismometer. The hydrophone is either an *E-2PD* hydrophone from *OAS Inc.* or a *HTI-01-PCA* hydrophone from *HIGH TECH Inc.* The sensitive seismometer is deployed between the anchor and the OBS frame, which allows good coupling with the seafloor. Geophones used for the OBS (Figure 4.1) had a natural frequency of 4.5 Hz. The three component seismometers from *KUM* GmbH are housed in a titanium tube, modified from a package built by Tim Owen (Cambridge). The signal of the sensors is recorded using *Marine Longtime Seismocorder (MLS)* or *Marine Tsunameter Seismocorder (MTS)*, which were manufactured by SEND GmbH and specially designed for long-time recordings of low frequency bands.

During the deployment on the seafloor the entire system rests horizontally on the anchor frame (Fig. 4.1). After releasing its anchor weight, however, the instrument turns 90° into the vertical and ascends to the surface with the floatation on top (Fig. 4.2). This ensures a maximally reduced system height and water current sensibility during deployment. Further, the sensors are well protected against damage during recovery and the transponder is kept under water, allowing permanent ranging, while the instrument floats at the surface.

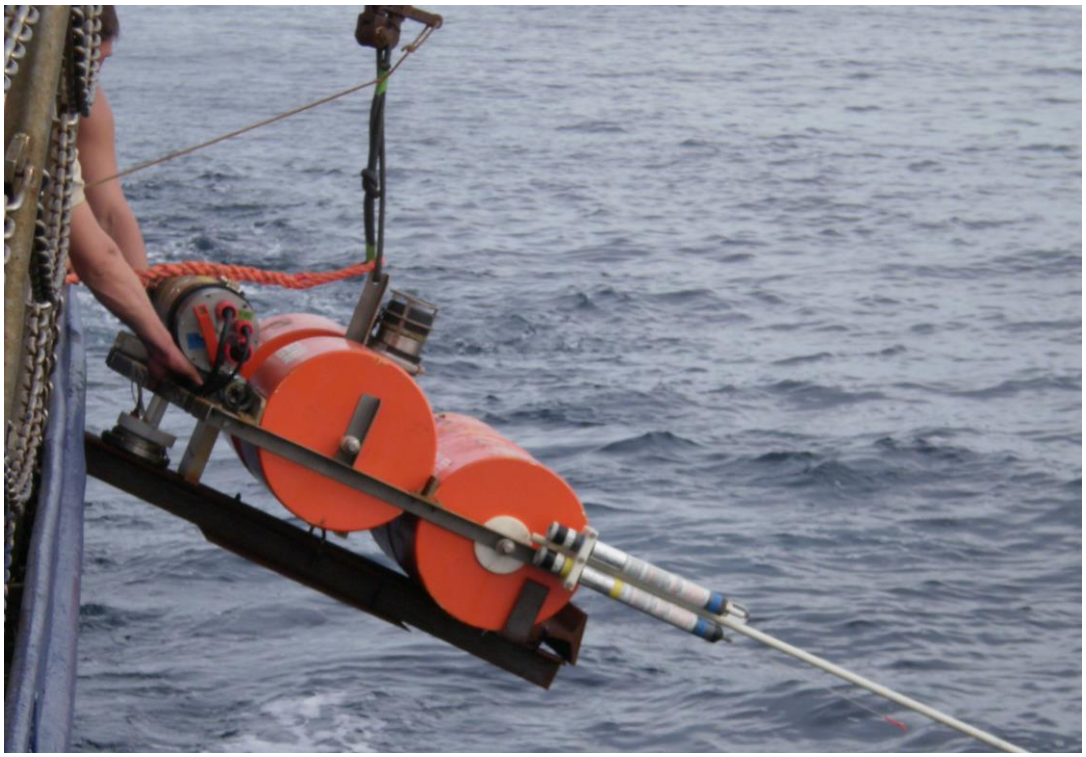

Figure 4.1 Short period OBS with 4.5 Hz seismometer before deployment from RV Poseidon

Recorder type	Internal time base drift [ppm]	No. channels	Sampling rate [Hz]	Resolution	Storage media	Power consumption [mW]	Application
MLS – Marine Longterm Seismocorder	<0.05	4	1-200	50 Hz: 19 bit	PCMCIA Flash disks	250	seismology
MTS – Marine Tsunameter Seismocorder	<0.05	5	1-200	50 Hz: 19 bit	PCMCIA Flash disks	250	seismology

Table 4.1. Performance of seismic recorders.

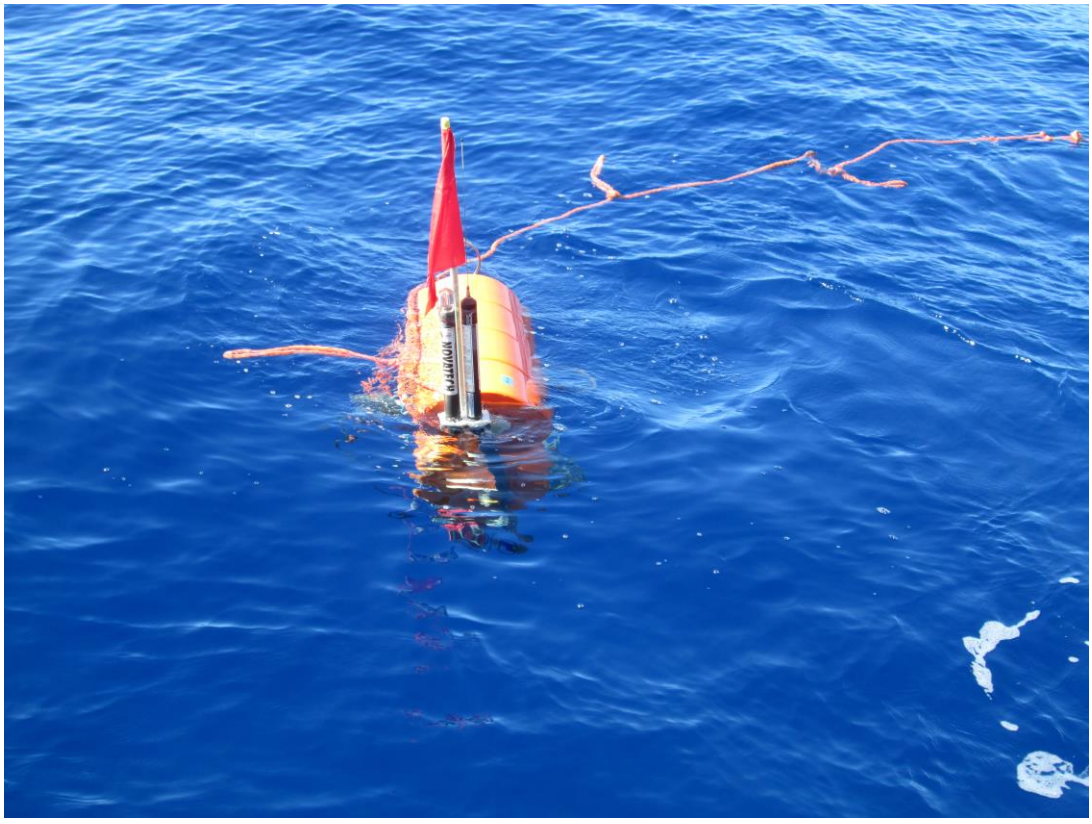

Figure 4.2 OBS floating at the sea-surface before recovery

5. Data quality and first results

5.1 Horesshoe Abyssal Plain (HASP) deployment

5.1.1 Local earthquakes in the HASP

The seismological network in the Horseshoe Abyssal Plain was operated between 14th of April 2012 and the 16th of October 2012 and hence over a period of about 6 month. The network was installed in the vicinity of the Horseshoe fault and cross cutting SWIM faults (Fig. 5.1.). Raw data stored on the recorders were converted to Pseudo-segy or PASSCAL-Segy format of IRIS using *SEND* software. To generate more manageable files sizes and for applying time corrections, the files were cut into 25 hours records with one hour overlap between adjacent records, such that each record generally begins at 0:00:01. For all stations timing errors of the internal clock against GPS time were corrected.

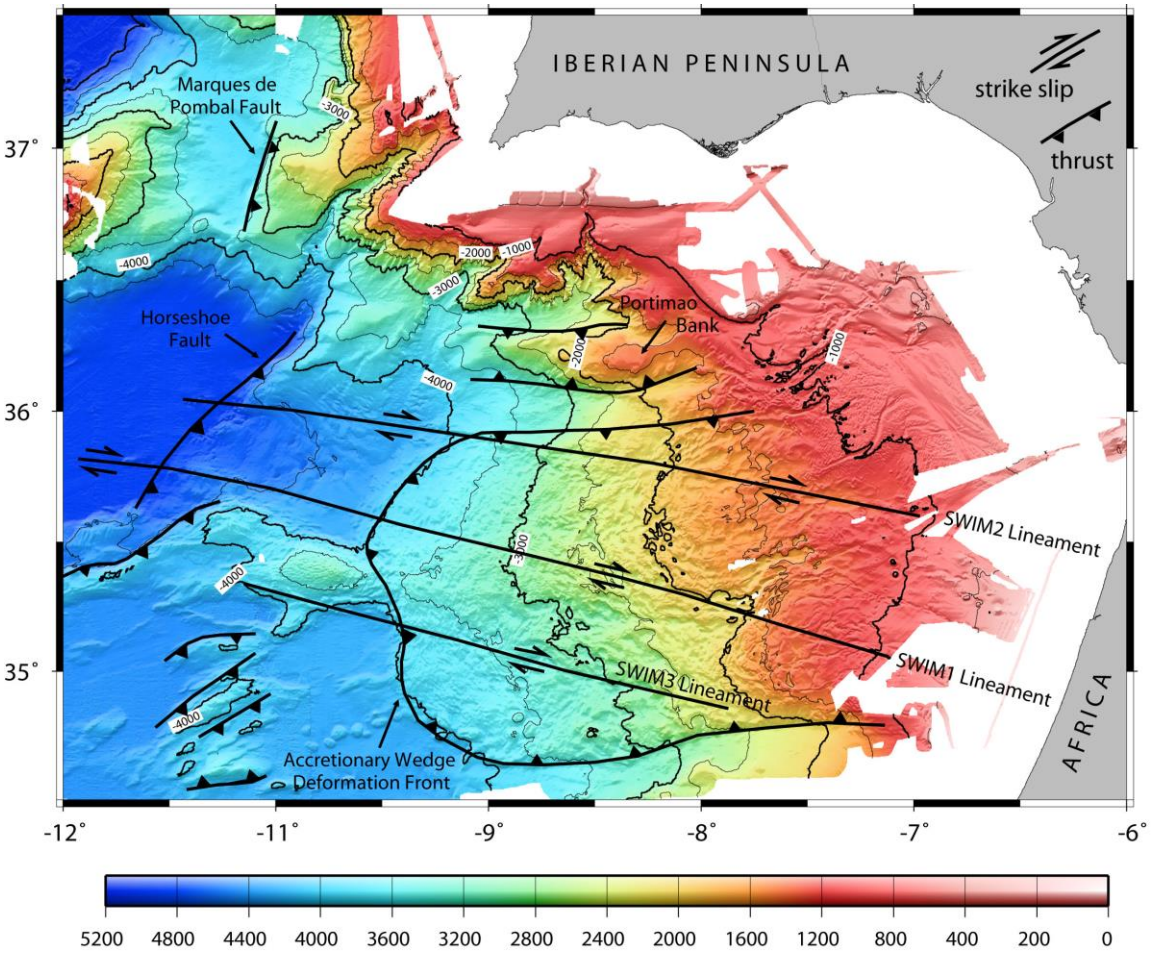

Figure 5.1. Main structural features identified in the Gulf of Cadiz (Zitellini et al., 2009).

To detect automatically seismic events in the daily records a short-term-average versus a long-term-average (STA/LTA) trigger algorithm was applied. The code used was REFTRIG from the IRIS PASSCAL program library. The trigger parameters include the length of the short term (s) and long term (l) time window, the mean removal window length (m), the trigger (t) and detrigger ratio (d), minimum number of stations (S) and the network trigger time window length (M). The trigger parameters were applied to unfiltered vertical component data. To test the trigger parameters a continuous 24 hours data stream of all stations is visually checked. Moreover, we tested the parameters for a number of days and transferred the data into the SEISAN package used to analyse and locate the local earthquakes. Applying

these trigger parameters we obtain less than ~10% false triggers and lose only those events that were recorded only on very few stations, while all major events are triggered.

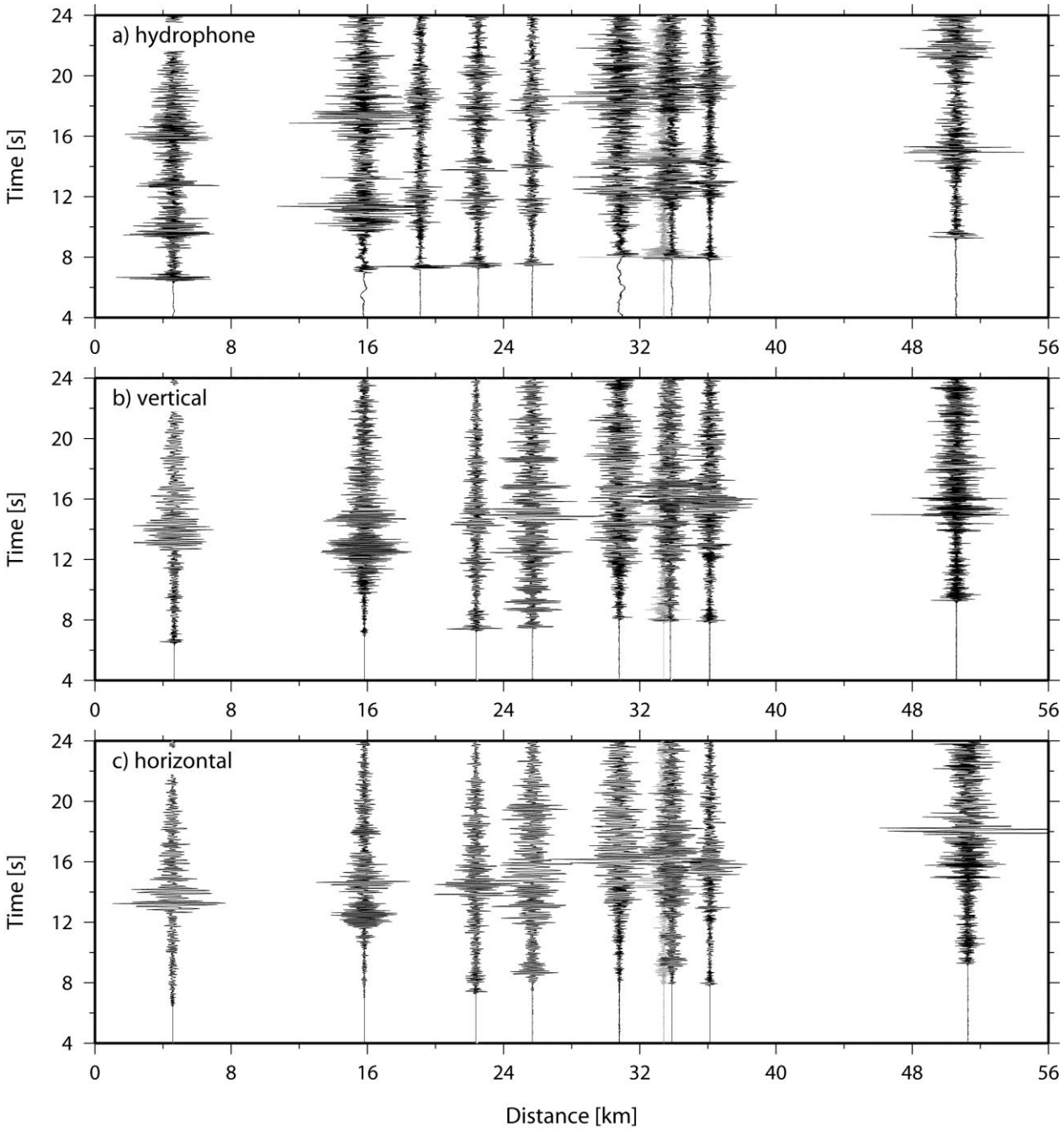

Fig. 5.2.Waveform example of a Ml=3.3 event recorded in the Horseshoe Abyssal Plain on 5th of July 2012, occurring at 56 km depth.

After finding event triggers, the events were cut from the 25 hours files and stored into subdirectories, one per event. Because we are investigating local earthquakes the appropriate time window length for the events is 3 minutes, starting 30 s prior to trigger time. The SEGY traces in the event directories are converted first into SAC, and then into MSEED waveform format, which makes it possible to store all traces associated with an event into a single waveform file. After conversion the data are registered into a

SEISAN database (*Havskov and Ottemöller*, 2005). *P*-wave and *S*-wave arrival times are picked and events are located using the non-linear probabilistic location procedure NonLinLoc of *Lomax et al.*

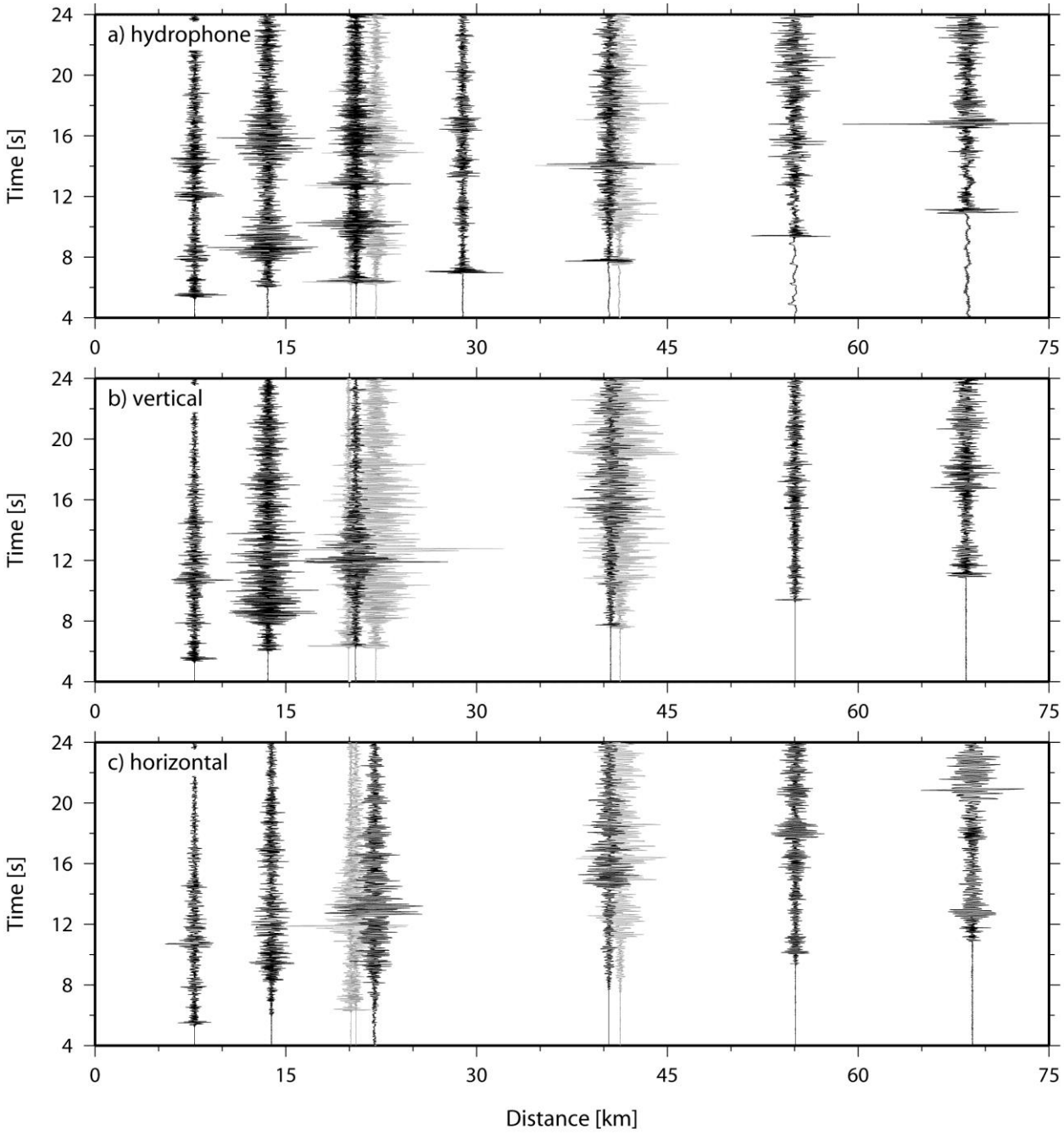

Fig. 5.3. Waveform example of a Ml=2.2 event recorded in the Horseshoe Abyssal Plain on 9th of July 2012, rupturing at 46 km.

(2000). Travel times are calculated using a 1-D velocity model base on the work of *Martinez-Loriente et al.* (2014). The velocity model consists of a number of layers, including sedimentary layers with velocities of 1.6 km/s to 3.8 km/s and a total thickness of 4 km. Below, velocities increase gradually from 5 km/s to 7.4 km/s over 4 km. Below 10 km a half space with upper mantle velocities of 8.0 km/s occurs. We used different parametrizations of the *Martinez-Loriente et al.* (2014) model to test its impact on hypocentre determination. However, re-locations were robust.

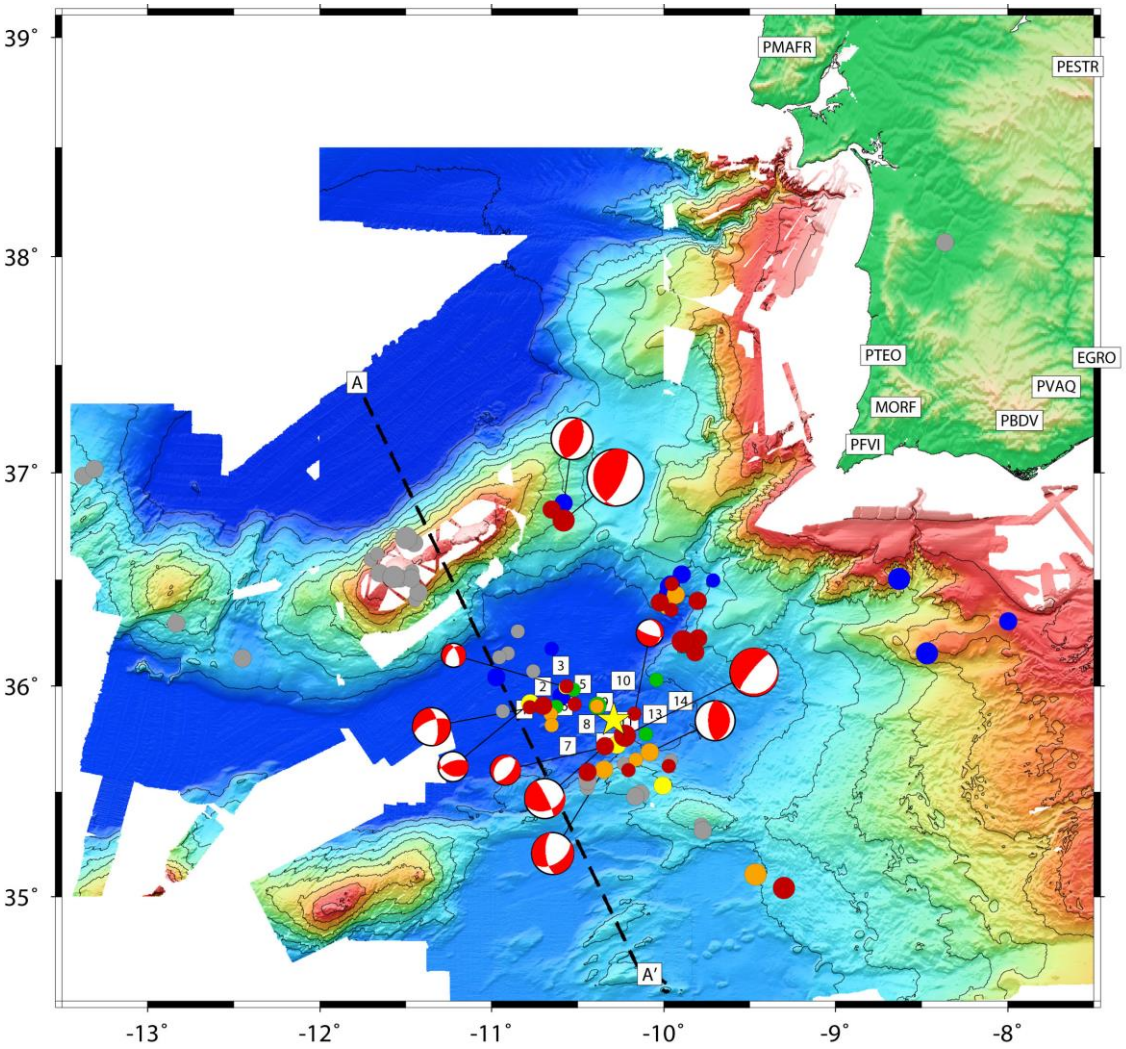

Figure 5.4. Earthquakes recorded with the offshore network in the vicinity of the Horseshoe Abyssal Plain. Earthquake magnitude scales with the size of the symbols (magnitude ~3.3 to 1.0); depth is coded by colour: blue < 10 km; green 10 km < z < 20 km, yellow 20 km < z < 30 km; orange 30 km < z < 40 km, red > 40 km. Light grey mark earthquakes were the gap was too large for a precise estimate of both epicentre and depth.

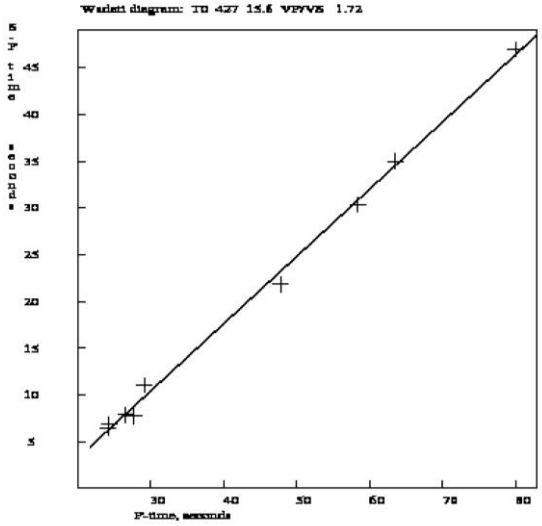

Fig. 5.5: Waditi Diagram, revealing a Vp/Vs ratio of 1.72 and hence indicating rather normal mantle conditions.

We detected 82 local earthquakes with good station coverage and at close distance to the network. The largest event with Ml=3.3 occurred on 5th of July 2012 at ~50 km depth. Waveform examples are given in Figure 5.2. Another example of a Ml=2.2 earthquake is given in Figure 5.3. To increase the coverage we did include permanent landstations from Portugal. Figure 5.3 shows all located earthquakes and onshore station included in the analysis. Additional stations at larger offsets are show as squares in Figure 1.1.

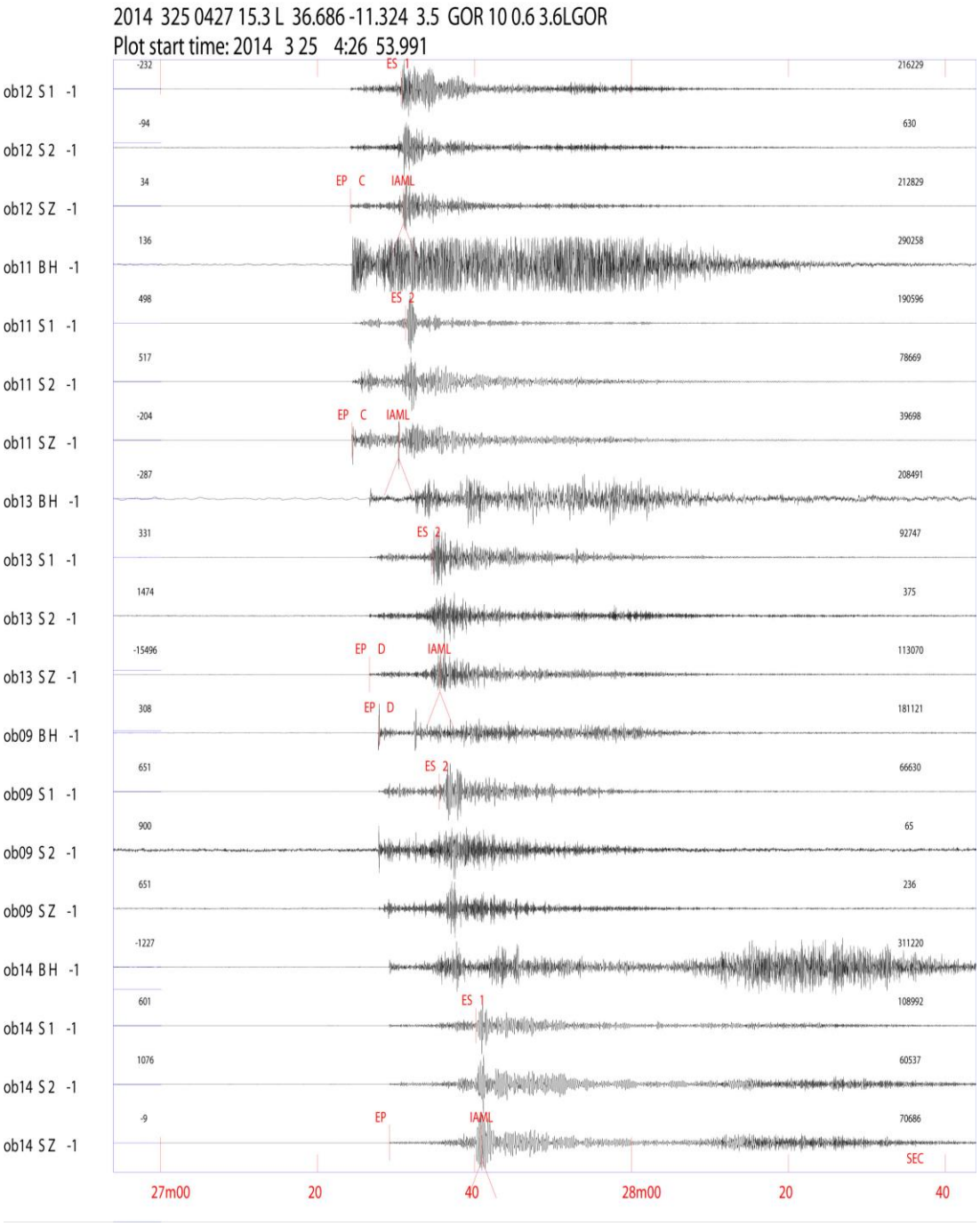

Figure 5.6. Waveform example of an Ml=3.6 event at the Gorringe Bank recorded on 25th of March 2014, while recovering the seismic network.

Earthquake epicentres correlate very weakly with any fault traces detected either in bathymetric data (like the SWIM faults) or in seismic reflection data. Thus, neither the NE-SW striking Horseshoe fault is outlines by increased levels of seismicity nor is the NNW-SSE striking SWIM 1 fault highlighted as a band of significant seismicity. However, some earthquakes occurring outside of the network in the vicinity of the Coral Patch Ridge may indicate activity of the SWIM faults. Due to the fact that the events occurred outside of the network any robust assessment is jeopardised by trade-offs between epicentral distances and source depth.

Source depth for events within the network is well-defined. Most events occurred at a depth of 30 to 50 km and hence within the mantle as the crust in the area occurs at <10 km below sea level (*Martinez-Loriente et al.*, 2014). Therefore, depth estimates are generally 10-15 km shallower then events reported by *Geissler et al.* (2010) for the same area. As discussed above (see chapter 2.2), the differences might be cause by the velocity model used by *Geissler et al.* (2010), which used a continental type velocity structure and thicker crust. Therefore, the maximum depth of seismic rupture occurs at ~50 km depth. Heat flow anomalies, however, would suggest that earthquakes in oceanic lithosphere should occur at temperature of <600°C and hence at <40 km. Earthquakes occurring at 50 km depth would suggest either that seismogenic rupture may occur at temperatures of >600°C or that heat flow anomalies are not caused in the mantle but at shallower level. For example, high values of radiogenic heat production of sediments flooring the Horseshoe Abyssal Plain could cause a higher surface heat flow. In this case lithospheric heat flow would be lower and hence could support faulting down to greater depth. In our initial models heat production has basically been neglected. Thus, if sediments accumulated in the Horseshoe Abyssal Plain would have a rather high heat production, for example reaching the highest values reported for some coastal provinces of Iberia (Fermandez et al., 1998), lithospheric heat flow could indeed be much lower and consequently earthquakes could occur at greater depth. This issue needs to be studied in much more detail.

The Horseshoe Abyssal Plain belongs to the same province forming today the Iberia Abyssal Plain (Rovere et al., 2004) and thus might be composed of unroofed continental mantle. Based on seismic velocities it has been discussed that the mantle might be serpentinized (*Rovere et al.*, 2004; *Martinez-Loriente et al.*, 2014). However, Wadati-diagrams indicate that Vp/Vs ratio is in the order of 1.72 (Fig. 5.5) and hence support normal mantle conditions; serpentinized mantle should have high Vp/Vs ratios of 1.9 to 2.2. Therefore, reduced P-wave velocity of the mantle might be caused by fracturing and faulting rather than alteration of peridotites.

5.2 Gorringe Bank depolyment

5.2.1 Local earthquakes at the Gorringe Bank

The seismological network at the Gorringe Bank was operated between 8th of October 2013and 25th of March 2014, monitoring seismicity in an area that has been discussed being the source of the Great Lisbon earthquake (Johnston, 1996). The data were analyses as described in 5.1.1. Surprisingly, only about 50 local earthquakes could be detected and only four additional events have been recorded that were not detected by the Portuguese seismic network. The largest event recorded had a magnitude of 3.6 and occurred while the seismic network was recovered (Fig. 5.6). For the location procedure we used two different velocity-depth models based on the seismic P-wave velocity model of *Martinez-Loriente et al.* (2014). One model characterized the Horseshoe Abyssal Plain and the other the top of the Gorringe Bank. Overall, source locations show only shall changes both in the and epicentral location, indicating that most earthquakes occurred at a depth of 20 to 30 km and hence shallower than in the Horseshoe Abyssal plain.

In map view the local earthquakes did not highlight any clear fault structures or preferred orientations (Fig. 5.7). Projected along the seismic profile and velocity model of *Martinez-Loriente et al.* (2014), we

could not identify any dipping fault or trend of faulting (Fig. 5.8). A very clear feature, however, is the fact that earthquakes at Gorringe Bank occurred at shallower depth compared to seismicity of the Horseshoe Abyssal Plain. However, both clusters of activity did not support a common feature, like a developing subduction thrust that has been previously discussed (Duarte et al., 2013).

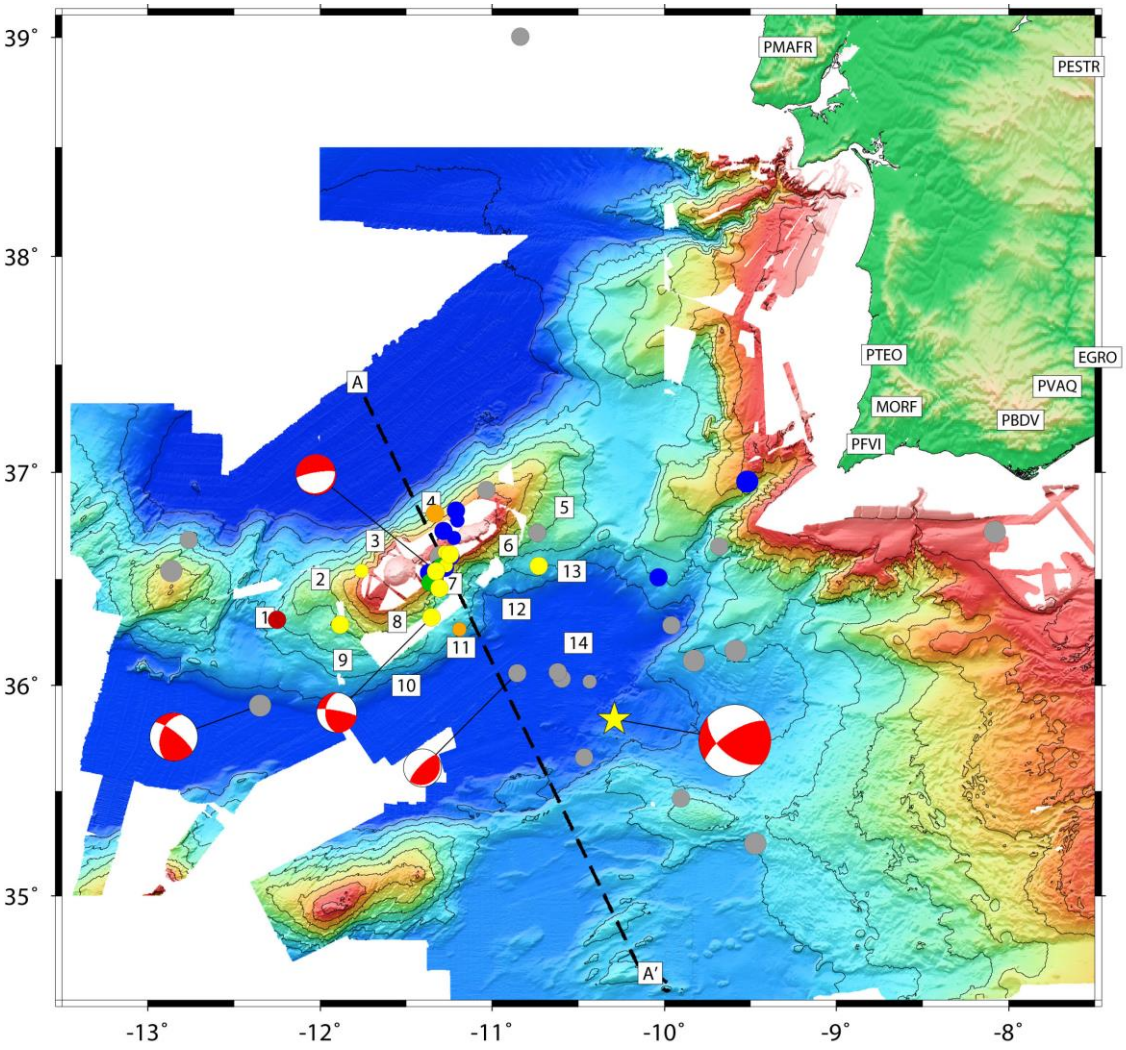

Figure 5.7. Earthquakes recorded with the network deployed at the Gorringe Bank. The dataset has been complemented by data from the onshore stations. Earthquake magnitude scales with the size of the symbols (magnitude ~3.6 to 1.5); depth is coded by colour: blue < 10 km; green 10 km < z < 20 km, yellow 20 km < z < 30 km; orange 30 km < z < 40 km, red > 40 km. Light grey mark earthquakes were the gap was too large for a precise estimate of both epicentre and depth. Yellow star is the epicenter of the Mw=6.0 Horseshoe earthquake.

5.3 Discussion – Assessment of goals

The data and data analyses presented in this report are based on a first assessment of the data, which are currently analyzed in much more detail. However, based on the results present we like to briefly discuss the results and observed features with respect to the goals of the study introduced in chapter 2.4.

1. Characterization of the minimum and maximum depth of local earthquakes

Precise estimates of earthquake locations (both in Lon/Lat and depth) will allow us to approximate the thickness of the seismogenic layer. In turn, this has important implications for the rheology and mechanical behavior of the lithosphere.

Both deployments provided a number of well-located earthquakes that will allow us to characterize with high precision hypocentral parameters. We believe, however, that features found so far are robust enough to indicate that faulting in the Horseshoe Abyssal Plain extends far down into the mantle and that the mantle is strong enough to support a large single fault plain that could produce a 1755 Lisbon-like earthquake.

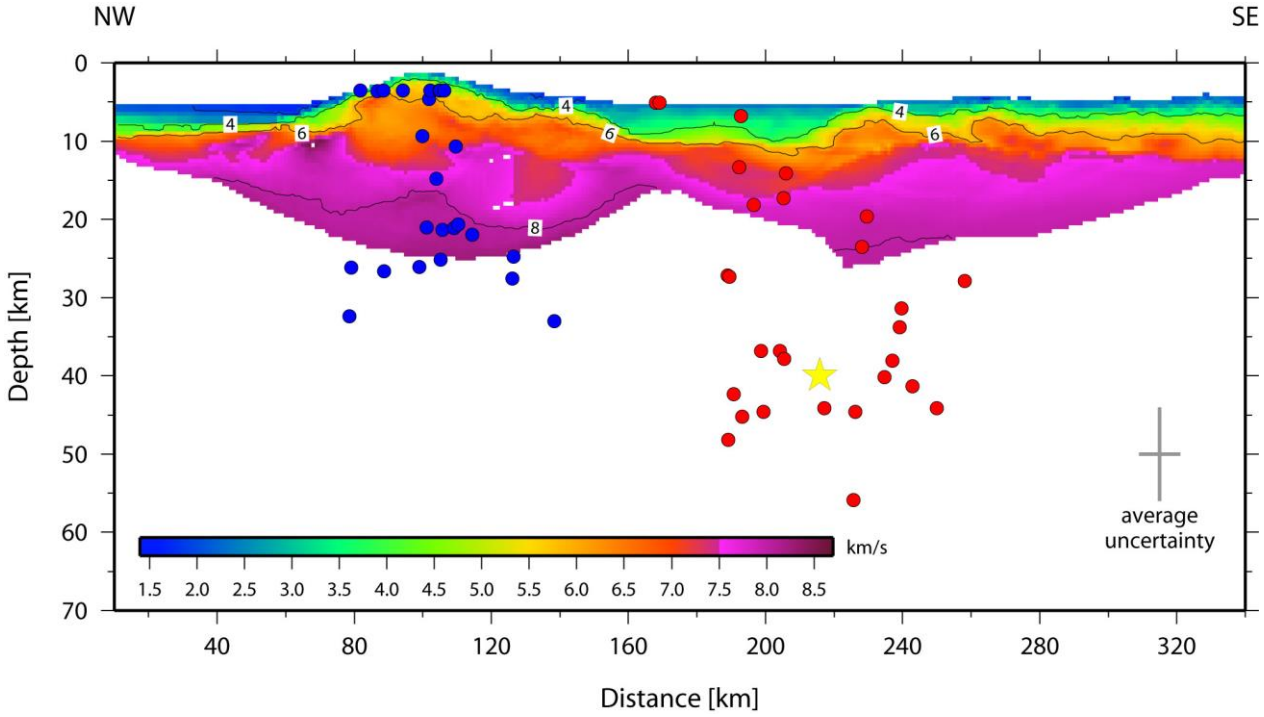

Figure 5.8. Earthquakes (+/- 30 km off the profile) projected onto the seismic profile of Martinez-Loriente et al. (2014).For location see profile AA' in Figs. 5.4 + 5.7. Events plotted in blue are from the Gorringe Bank deployment, red indicates events from the Horseshoe Abyssal Plain deployment and yellow star is the hypocentre of the Mw=6.0 2007 Horseshoe Earthquake.

2. Defining frequency-magnitude relationship for Horseshoe earthquakes

The so called b-value can be used to understand and survey the frequency-size distribution of earthquakes. In the case of wide-spread serpentinization, a high b-value of >~2 might be expected, as found for bending-related earthquakes in the trench-outer rise of subduction zones (Lefeldt et al., 2009). A b-value of ~1 would indicate normal conditions.

Robust statistical parameters have not been defined yet. However, even the relatively small number of earthquakes can be used to provide an initial assessment of the *b*-values. Preliminary calculations indicate low *b*-values in the order of 0.5 to 0.6 for both networks.

3. Characterization of the seismic velocity structure of the Horseshoe Abyssal Plain using P- and S-waves

A large number of local earthquakes recorded on a local network can be used to invert the travel time data jointly for earthquake location and a so called minimum 1-D velocity model. If the number of local events is large enough, a 3-D velocity structure can be derived. Right now, existing active source data could not penetrate deeper than ~11 to 13 km and are limited in their ability to derive S-wave velocities. However, using P- and S-wave arrival times of local earthquakes the velocity structure can be resolved at

larger depth, as earthquakes nucleate at least down to 35-40 km, as indicated by the Mw=6.0 Horseshoe earthquake. The Vp/Vs ratio is important for assessing the amount of serpentinization.
The number of earthquakes detected during both deployments was much smaller than expected. It might therefore be difficult to derive a robust and well-resolved reference or minimum 1D model. However, Wadati-diagrams can be used to provide an initial assessment of Vp/Vs ratios (see Fig. 5.5).

4. Surveying the relationship between maximum depth of seismic activity and thermal structure
Previous estimates for oceanic lithosphere suggest that faulting is limited to temperatures of <600°C. It has been proposed that the rocks underlying the Horseshoe Abyssal Plain are unroofed continental lithosphere. Does this relationship also apply for continental mantle?
We briefly discussed this issue in section 5.1.1. The source depth of earthquakes down to 50 km would correspond to a surface heat flow of 45 mW/m2. However, surface heat flow was in the order of 60 mW/m2 and hence would suggest that earthquakes either occur at temperatures >600 °C or that thermal models are inaccurate. Therefore, we need to survey realistic thermal parameters more carefully as some sediments derived from Iberia were reported having rather high heat production values, which could explain the observe d bias.

5. Estimation of the strength of the lithosphere in the Horseshoe Abyssal Plain to assess the seismic hazard of a future large earthquake
The assessment of the b-value and the Vp/Vs ratio will provide a first assessment for the rheology and of a strong or weak mantle. The strength of the host rock is important for the frictional properties of a fault zone. In addition to the size (define by the thickness of the seismogenic layer and the length of a fault) the frictional behavior will govern the seismic moment of a future earthquake.
Indeed, the mantle in the Horseshoe Abyssal Plain seems to be strong enough to support earthquakes down to 50 km, supporting a strong mantle and the potential for large (M~7) to great (M~8) future earthquakes.

6. Using focal mechanism to define fault segments
Seismic reflection data revealed a number of fault zones in the Horseshoe abyssal plain. Focal mechanisms can be used to assess motion of these faults.
Initial focal mechanisms were calculated using first motions polarities of the OBS data (Fig. 5.4 + 5.7). However, additional polarities from land seismometers have to be included to support focal mechanisms.

7. Earthquake activity and seepage
In the vicinity of the Horseshoe faults seepage and mud volcanoes were observed. It is likely that seepage will occur over active faults. The densely spaced OBS network might be able to located some local earthquakes or clusters of events that are related to faults governing fluid migration.
Unfortunately, the number of earthquake along SWIM faults is much too small and events did not cluster at locations of seepage to support a relationship been seismicity and fluid migration. However, the monitoring period might have been too short considering the small *b*-values of <1 to study such a relationships.

6. Acknowledgements

The sea-going programme was funded by the German Science Foundation (DFG) through the grant GR1964/15-1 and the GEOMAR Helmholtz Centre for Ocean Research Kiel though it OCEANS programme. We acknowledge the excellent and professional sea-going operation of R/V *Poseidon* by Captains Matthias Günther and Bernhard Windscheid and their crews. Further, we acknowledge support from Luis Mattias from Lisbon University.

7. References

Argus, D.F., Gordon, R.G., Demets, C., Stein, S. Closure of the Africa–Eurasia–North America plate motion circuit and tectonics of the Gloria fault. J. Geophys. Res. 94, 5585–5602, 1989

Baptista, M.A., Heitor, S., Miranda, J.M., Miranda, P.M.A., Mendes Victor, L., The 1755 Lisbon; evaluation of the tsunami parameters. J. Geodyn. 25, 143–157, 1998.

Buforn, E., Bezzeghoud, M., Udías, A. and Pro, C., 2004. Seismic Sources on the Iberia-African Plate Boundary and their Tectonic Implications. Pure Appl. Geophys., 161(3), 623-646.

Delescluse, M., Chamot-Rooke, N., Serpentinization pulse in the actively deforming Central Indian Basin, Earth Planet. Sci. Lett. 276, 140–151, 2008.

Duarte J. C., Terrinha P., Rosas F. M., Valadares V., Pinheiro L. M., Matias L., Magalhães V., Roque, C., Crescent-shaped morphotectonic features in the Gulf of Cadiz (offshore SW Iberia). Marine Geology 271, 236-249, 2009.

Duarte, J.C., F.M. Rosas, P. Terrinha, W.P. Schellart, D. Boutelier, M.-A. Gutscher, A. Ribeiro, Are subduction zones invading the Atlantic? Evidence from the southwest Iberia margin, Geology, 41, 839-842, doi:10.1130/G34100.1, 2013.

Engdahl, R., R. van der Hilst, and R. Buland, Global teleseismic earthquake relocation with improved traveltimes and procedures for depth determination, Bull. Seismol. Soc. Am., 88, 722–743, 1998.

Fernàndez, M., I. Marzán, A. Correia, and E. Ramalho, Heat flow, heat production, and lithospheric thermal regime in the Iberian Peninsula. Tectonophysics, 291, 29–53, 1998.

Fukao, Y., 1973. Thrust faulting at a lithospheric plate boundary: The Portugal earthquake of 1969. Earth Planet. Sci. Lett., 18, 205–216.

Geissler, W. H., L. Matias,2D. Stich, F. Carrilho, W. Jokat, S. Monna, A. IbenBrahim, F. Mancilla, M.-A. Gutscher, V. Sallarès, and N. Zitellini, Focal mechanisms for sub-crustal earthquakes in the Gulf of Cadiz from a dense OBS deployment, Geophys. Res. Lett., 37, doi:10.1029/2010GL044289, 2010.

González, A., M. Torné, D. Córdoba, N. Vidal, L. M. Matias, and J. Díaz, Crustal thinning in the southwestern Iberia margin, Geophys. Res. Lett., 23, 2477–2480, doi:10.1029/96GL02299, 1996.

Gracia, E., Danobeitia, J.J., Verges, J., PARSIFAL Team, 2003. Mapping active faults offshore Portugal (36°N–38°N): implications for seismic hazard assessment along the southwest Iberian margin. Geology 31, 83–86.

Grevemeyer, I., C.R. Ranero, E.R. Flueh, D. Klaeschen, J. Bialas, Passive and active seismological study of bending-related faulting and mantle serpentinization at the Middle America trench. Earth Planet. Sci. Lett., 258, 528-542, 2007.

Grevemeyer, I., Kaul, N., Kopf, A., Heat flow anomalies in the Gulf of Cadiz and off Cape San Vincente, Portugal, Mar. Petrol. Geol., 26, 795-804, doi:10.1016/j.marpetgeo.2008.08.006, 2009.

Gutscher, M.-A., Malod, J., Rehault, J.-P., Contrucci, I., Klingelhoefer, F., Mendes-Victor, L., Spakman, W., 2002. Evidence for active subduction beneath Gibraltar. Geology 30, 1071–1074.

Gutscher, M.-A., Baptista, M.A., Miranda, J.M., 2006. The Gibraltar Arc seismogenic zone: Part 2. Constraints on a shallow east dipping fault plane source for the 1755 Lisbon earthquake provided by tsunami modeling and seismic intensity. Tectonophysics 426, 153–166.

Havskov, J., and L. Ottemöller , Seisan: The earthquake analysis software for Windows, Solaris and Linux, version 7.2, technical report, Inst. of Solid Earth Phys., Univ. of Bergen, Bergen, Norway, 2001.

Hensen C., Nuzzo M., Hornibrook E. R. C., Pinheiro L. M., Bock F., Magalhães V. H., and Brueckmann W., Sources of mud volcano fluids in the Gulf of Cadiz - Indications for hydrothermal imprint. Geochimica et Cosmochimica Acta 71, 1232-1248, 2007.

Hayward, N., Watts, A.B., Westbrook, G.K., Collier, J.S., A seismic reflection and GLORIA study of compressional deformation in the Gorringe Bank region, eastern North Atlantic. Geophys. J. Int. 138, 831–850, 1999.

Johnston, A., 1996. Seismic moment assessment of earthquakes in stable continental regions — III. New Madrid, 1811–1812, Charleston 1886 and Lisbon 1755. Geophys. J. Int. 126, 314–344.

Lomax, A., Virieux, A. J., Volant, P., Berge, C., Probabilistic earthquake location in 3D and layered models: Introduction of a Metropolis-Gibbs method and comparison with linear locations, in Advances in Seismic Event Location, pp. 101-134, eds. Thurber, C. H. and Rabinowitz, N., Kluwer, Amsterdam., 2000.

Lefeldt, M., I. Grevemeyer, Centroid depth and mechanism of trench-outer rise earthquakes, Geophys. J. Int., 172, 240-251, 2008.

Lefeldt, M., I. Grevemeyer, J. Goßler, J. Bialas, Intraplate seismicity and related mantle hydration at the Nicaraguan trench-outer rise, Geophys. J. Int., 178, 742-752, doi:10.1111/j.1365-246X.2009.04167.x, 2009.

Lomax, A., J. Virieux, P. Volant and C. Thierry-Berge, Probabilistic earthquake location in 3D and layered models, in Advances in Seismic Event Location, pp. 101–134, eds Thurber, C.H. & Rabinowitz, N., Kluwer, Dordrecht, 2000.

Louden, K.E., J.-C. Sibuet, F. Harmegnies, Variations in heat flow across the ocean-continent transitioln in the Iberia abyssal plain, Earth Planet. Sci. Lett., 151, 233-254, 1997.

Kennett, B. L. N., E. R. Engdahl, and R. Buland, Constraints on seismic velocities in the Earth from traveltimes, Geophys. J. Int., 122(1), 108-124, doi:10.1111/j.1365-246X.1995.tb03540.x, 1995.

Kikuchi, M., and H. Kanamori, Inversion of complex body waves-III, Bull. Seismol. Soc. Am., 81(6), 2335-2350, 1991.

Kikuchi, M., and M. Ishida, Source retrieval for deep local earthquakes with broadband records, Bull. Seismol. Soc. Am., 83(6), 1855-1870, 1993.

Martinez-Loriente, S., et al. Seismic and gravity constraints on the nature of the basement in the Africa-Eurasia plate boundary: New insights for the geodynamic evolution of the SW Iberian margin, J. Geophysical Research, 119, 127-149, doi: 10.1002/2013JB010476, 2014.

Martinez-Solares, J.M., Lopez, A., Mezcua, J., 1979. Isoseismal map of the 1755 Lisbon earthquake obtained from Spanish data. Tectonophysics 53, 301–313.

McKenzie, D., J. Jackson, and K. Priestley (2005), Thermal structure of oceanic and continental lithosphere, Earth Planet. Sci. Lett., 233, 337–349, doi:10.1016/j.epsl.2005.02.005, 2005.

Moore J. C. and Vrolik P., Fluids in accretionary prisms. Reviews of Geophysics 30, 113-135, 1992.

Müller R.D., Sdrolias M., Gaina C. and Roest W.R., Age, spreading rates, and spreading asymmetry of the world's ocean crust. Geochemistry, Geophysics, Geosystems 9, Q04006, doi:10.1029/2007GC001743, 2008.

Sartori, R., Torelli, L., Zitellini, N., Peis, D., Lodolo, E., 1994. Eastern segment of the Azores–Gibraltar line (central-eastern Atlantic): an oceanic plate boundary with diffuse compressional deformation. Geology 22, 555–558.

Rosas F. M., Duarte J. C., Terrinha P., Valadares V., and Matias L, Morphotectonic characterization of major bathymetric lineaments in Gulf of Cadiz (Africa-Iberia plate boundary): Insights from analogue modelling experiments. Mar. Geol. 261, 33-47, 2009.

Rovere,M., C.R. Ranero, R. Sartori, L. Torelli, N. Zitellini, Seismic images and magnetic signature of the Late Jurassic to Early Cretaceous Africa–Eurasia plate boundary off SW Iberia, Geophys. J. Int., 158, 554–568, 2004.

Scholz F., Hensen C., Reitz A., Romer R.L., Liebetrau V., Meixner A., Weise S.M. and Haeckel M., Isotopic evidence (87Sr/86Sr, □7Li) for alteration of the oceanic crust at deep-rooted mud volcanoes in the Gulf of Cadiz, NE Atlantic Ocean. Geochimica et Cosmochimica Acta 73, 5444-5459, 2009.

Stich, D., F. Mancilla, S. Pondrelli, and J. Morales, Source analysis of the February 12th 2007, Mw 6.0 Horseshoe earthquake: Implications for the 1755 Lisbon earthquake, Geophys. Res. Lett., 34, doi:10.1029/2007GL030012, 2007.

Waldhauser, F., and W. L. Ellsworth, A double-difference earthquake location algorithm: method and application to the northern Hayward fault, California, Bull. Seism. Soc. Am., 90, 1353-1368, 2000.

Wiens D. A., DeMets C., Gordon R. G., Stein S., Argus D., Engeln J. F., Lundgren P., Quible D., Weinstein S., and Woods D. F., A diffuse plate boundary model for the Indian Ocean Tectonics. Geophysical Research Journal 12(7), 429-432, 1985.

Zitellini, N., et al., 2001. Source of 1755 Lisbon earthquake and tsunami investigated. EOS, 82, 285–291.

Zitellini N., Gràcia E., Matias L., Terrinha P., Abreu M.A., De Alteriis G., Henriet J.P., Dañobeitia J.J., Masson D.G., Mulder T., Ramella R., Somoza L. and Diez S. (2009). The quest for the Africa-Eurasia plate boundary west of the Strait of Gibraltar. Earth Planet. Sci. Lett., 280, 13-50, 2009.

Appendix I

8.1 – Station List Horesshoe Abyssal Plain deployment

Station name	Latitude	Longitude	Water depth [m]
OBS01	35° 53,31' N	10° 48,68' W	4815
OBS02	35° 59,90' N	10° 42,25' W	4828
OBS03	36° 5,78' N	10° 35,84' W	4799
OBS04	36° 11,99' N	10° 29,34' W	4796
OBS05	36° 0,56' N	10° 28,21' W	4794
OBS06	35° 54,40' N	10° 34,64' W	4790
OBS07	35° 42,99' N	10° 33,45' W	4804
OBS08	35° 49,20' N	10° 26,95' W	4804
OBS09	35° 55,42' N	10° 20,55' W	4802
OBS10	36° 1,56' N	10° 14,13' W	4837
OBS11	35° 50,16' N	10° 12,88' W	4643
OBS12	35° 43,96' N	10° 19,33' W	4524
OBS13	35° 52,07' N	10° 2,99' W	4570
OBS14	35° 55,77' N	9° 54,11' W	4500

Appendix II

8.2 – Station List Gorringe Bank deployment

Station	Latitude	Longitude	Water depth [m]	comment
OBS01	36° 19.14' N	12° 19,20' W	3876	
OBS02	36° 30.00' N	12° 00.00' W	2970	
OBS03	36° 40.81' N	11° 40.70' W	3258	
OBS04	36° 51.55' N	11° 21.36' W	3555	
OBS05	36° 50.20' N	10° 34.90' W	3083	
OBS06	36° 39.50' N	10° 54.40' W	2655	
OBS07	36° 28.80' N	11° 13.78 ' W	2848	
OBS08	36° 18.03' N	11° 33.10' W	2233	
OBS09	36° 07.16' N	11° 52.14' W	3491	
OBS10	35° 59.99' N	11° 29.98' W	4766	
OBS11	36° 10.81' N	11° 10.85' W	4561	
OBS12	36° 21.55' N	10° 51.62' W	4692	
OBS13	36° 32.27' N	10° 32.25' W	4349	
OBS14	36° 12.01' N	10° 30.01' W	4794	
OBS15	35° 48.99’ N	10° 40.02’ W	4757	lost at sea

GEOMAR
Helmholtz-Zentrum für Ozeanforschung Kiel

GEOMAR Reports

No.	Title
1	FS POSEIDON Fahrtbericht / Cruise Report POS421, 08. – 18.11.2011, Kiel - Las Palmas, Ed.: T.J. Müller, 26 pp, DOI: 10.3289/GEOMAR_REP_NS_1_2012
2	Nitrous Oxide Time Series Measurements off Peru – A Collaboration between SFB 754 and IMARPE –, Annual Report 2011, Eds.: Baustian, T., M. Graco, H.W. Bange, G. Flores, J. Ledesma, M. Sarmiento, V. Leon, C. Robles, O. Moron, 20 pp, DOI: 10.3289/GEOMAR_REP_NS_2_2012
3	FS POSEIDON Fahrtbericht / Cruise Report POS427 – Fluid emissions from mud volcanoes, cold seeps and fluid circulation at the Don-_Kuban deep sea fan (Kerch peninsula, Crimea, Black Sea) – 23.02. – 19.03.2012, Burgas, Bulgaria - Heraklion, Greece, Ed.: J. Bialas, 32 pp, DOI: 10.3289/GEOMAR_REP_NS_3_2012
4	RV CELTIC EXPLORER EUROFLEETS Cruise Report, CE12010 – ECO2@NorthSea, 20.07. – 06.08.2012, Bremerhaven – Hamburg, Eds.: P. Linke et al., 65 pp, DOI: 10.3289/GEOMAR_REP_NS_4_2012
5	RV PELAGIA Fahrtbericht / Cruise Report 64PE350/64PE351 – JEDDAH-TRANSECT -, 08.03. – 05.04.2012, Jeddah – Jeddah, 06.04 - 22.04.2012, Jeddah – Duba, Eds.: M. Schmidt, R. Al-Farawati, A. Al-Aidaroos, B. Kürten and the shipboard scientific party, 154 pp, DOI: 10.3289/GEOMAR_REP_NS_5_2013
6	RV SONNE Fahrtbericht / Cruise Report SO225 - MANIHIKI II Leg 2 The Manihiki Plateau - Origin, Structure and Effects of Oceanic Plateaus and Pleistocene Dynamic of the West Pacific Warm Water Pool, 19.11.2012 - 06.01.2013 Suva / Fiji – Auckland / New Zealand, Eds.: R. Werner, D. Nürnberg, and F. Hauff and the shipboard scientific party, 176 pp, DOI: 10.3289/GEOMAR_REP_NS_6_2013
7	RV SONNE Fahrtbericht / Cruise Report SO226 – CHRIMP CHatham RIse Methane Pockmarks, 07.01. - 06.02.2013 / Auckland – Lyttleton & 07.02. – 01.03.2013 / Lyttleton – Wellington, Eds.: Jörg Bialas / Ingo Klaucke / Jasmin Mögeltönder, 126 pp, DOI: 10.3289/GEOMAR_REP_NS_7_2013
8	The SUGAR Toolbox - A library of numerical algorithms and data for modelling of gas hydrate systems and marine environments, Eds.: Elke Kossel, Nikolaus Bigalke, Elena Piñero, Matthias Haeckel, 168 pp, DOI: 10.3289/GEOMAR_REP_NS_8_2013
9	RV ALKOR Fahrtbericht / Cruise Report AL412, 22.03.-08.04.2013, Kiel – Kiel. Eds: Peter Linke and the shipboard scientific party, 38 pp, DOI: 10.3289/GEOMAR_REP_NS_9_2013
10	Literaturrecherche, Aus- und Bewertung der Datenbasis zur Meerforelle (*Salmo trutta trutta L.*) Grundlage für ein Projekt zur Optimierung des Meerforellenmanagements in Schleswig-Holstein. Eds.: Christoph Petereit, Thorsten Reusch, Jan Dierking, Albrecht Hahn, 158 pp, DOI: 10.3289/GEOMAR_REP_NS_10_2013
11	RV SONNE Fahrtbericht / Cruise Report SO227 TAIFLUX, 02.04. – 02.05.2013, Kaohsiung – Kaohsiung (Taiwan), Christian Berndt, 105 pp, DOI: 10.3289/GEOMAR_REP_NS_11_2013

GEOMAR
Helmholtz-Zentrum für Ozeanforschung Kiel

No.	Title
12	RV SONNE Fahrtbericht / Cruise Report SO218 SHIVA (Stratospheric Ozone: Halogens in a Varying Atmosphere), 15.-29.11.2011, Singapore - Manila, Philippines, Part 1: SO218- SHIVA Summary Report (in German), Part 2: SO218- SHIVA English reports of participating groups, Eds.: Birgit Quack & Kirstin Krüger, 119 pp, DOI: 10.3289/GEOMAR_REP_NS_12_2013
13	KIEL276 Time Series Data from Moored Current Meters. Madeira Abyssal Plain, 33°N, 22°W, 5285 m water depth, March 1980 – April 2011. Background Information and Data Compilation. Eds.: Thomas J. Müller and Joanna J. Waniek, 239 pp, DOI: 10.3289/GEOMAR_REP_NS_13_2013
14	RV POSEIDON Fahrtbericht / Cruise Report POS457: ICELAND HAZARDS Volcanic Risks from Iceland and Climate Change:The Late Quaternary to Anthropogene Development Reykjavík / Iceland – Galway / Ireland, 7.-22. August 2013. Eds.: Reinhard Werner, Dirk Nürnberg and the shipboard scientific party, 88 pp, DOI: 10.3289/GEOMAR_REP_NS_14_2014
15	RV MARIA S. MERIAN Fahrtbericht / Cruise Report MSM-34 / 1 & 2, SUGAR Site, Varna – Varna, 06.12.13 – 16.01.14. Eds: Jörg Bialas, Ingo Klaucke, Matthias Haeckel, 111 pp, DOI: 10.3289/GEOMAR_REP_NS_15_2014
16	RV POSEIDON Fahrtbericht / Cruise Report POS 442, "AUVinTYS" High-resolution geological investigations of hydrothermal sites in the Tyrrhenian Sea using the AUV "Abyss", 31.10. – 09.11.12, Messina – Messina, Ed.: Sven Petersen, 32 pp, DOI: 10.3289/GEOMAR_REP_NS_16_2014
17	RV SONNE, Fahrtbericht / Cruise Report, SO 234/1, "SPACES": Science or the Assessment of Complex Earth System Processes, 22.06. – 06.07.2014, Walvis Bay / Namibia - Durban / South Africa, Eds.: Reinhard Werner and Hans-Joachim Wagner and the shipbord scientific party, 44 pp, DOI: 10.3289/GEOMAR_REP_NS_17_2014
18	RV POSEIDON Fahrtbericht / Cruise Report POS 453 & 458, "COMM3D", Crustal Structure and Ocean Mixing observed with 3D Seismic Measurements, 20.05. – 12.06.2013 (POS453), Galway, Ireland – Vigo, Portugal, 24.09. – 17.10.2013 (POS458), Vigo, Portugal – Vigo, Portugal, Eds.: Cord Papenberg and Dirk Klaeschen, 66 pp, DOI: 10.3289/GEOMAR_REP_NS_18_2014
19	RV POSEIDON, Fahrtbericht / Cruise Report, POS469, "PANAREA", 02. – 22.05.2014, (Bari, Italy – Malaga, Spain) & Panarea shallow-water diving campaign, 10. – 19.05.2014, Ed.: Peter Linke, 55 pp, DOI: 10.3289/GEOMAR_REP_NS_19_2014
20	RV SONNE Fahrtbericht / Cruise Report SO234-2, 08.-20.07.2014, Durban, South Africa - Port Louis, Mauritius, Eds.: Kirstin Krüger, Birgit Quack and Christa Marandino, 95 pp, DOI: 10.3289/GEOMAR_REP_NS_20_2014
21	RV SONNE Fahrtbericht / Cruise Report SO235, 23.07.-07.08.2014, Port Louis, Mauritius to Malé, Maldives, Eds.: Kirstin Krüger, Birgit Quack and Christa Marandino, 76 pp, DOI: 10.3289/GEOMAR_REP_NS_21_2014

GEOMAR
Helmholtz-Zentrum für Ozeanforschung Kiel

No.	Title
22	RV SONNE Fahrtbericht / Cruise Report SO233 WALVIS II, 14.05-21.06.2014, Cape Town, South Africa - Walvis Bay, Namibia, Eds.: Kaj Hoernle, Reinhard Werner, and Carsten Luter, 153 pp, DOI: 10.3289/GEOMAR_REP_NS_22_2014
23	RV SONNE Fahrtbericht / Cruise Report SO237 Vema-TRANSIT Bathymetry of the Vema-Fracture Zone and Puerto Rico TRench and Abyssal AtlaNtic BiodiverSITy Study, Las Palmas (Spain) - Santo Domingo (Dom. Rep.) 14.12.14 - 26.01.15, Ed.: Colin W. Devey, 130 pp, DOI: 10.3289/GEOMAR_REP_NS_23_2015

For GEOMAR Reports, please visit:
https://oceanrep.geomar.de/view/series/GEOMAR_Report.html

Reports of the former IFM-GEOMAR series can be found under:
https://oceanrep.geomar.de/view/series/IFM-GEOMAR_Report.html

GEOMAR
Helmholtz-Zentrum für Ozeanforschung Kiel

Das GEOMAR Helmholtz-Zentrum für Ozeanforschung Kiel
ist Mitglied der Helmholtz-Gemeinschaft
Deutscher Forschungszentren e.V.

The GEOMAR Helmholtz Centre for Ocean Research Kiel
is a member of the Helmholtz Association of
German Research Centres

Helmholtz-Zentrum für Ozeanforschung Kiel / Helmholtz Centre for Ocean Research Kiel
GEOMAR
Dienstgebäude Westufer / West Shore Building
Düsternbrooker Weg 20
D-24105 Kiel
Germany

Helmholtz-Zentrum für Ozeanforschung Kiel / Helmholtz Centre for Ocean Research Kiel
GEOMAR
Dienstgebäude Ostufer / East Shore Building
Wischhofstr. 1-3
D-24148 Kiel
Germany

Tel.: +49 431 600-0
Fax: +49 431 600-2805
www.geomar.de